Hydrodynamical simulations of galaxy formation

Volker Springel

- Old problems and recent progress in disk galaxy formation simulations

- Recent modelling additions: Magnetic fields and cosmic rays

- Anisotropic transport on a moving mesh

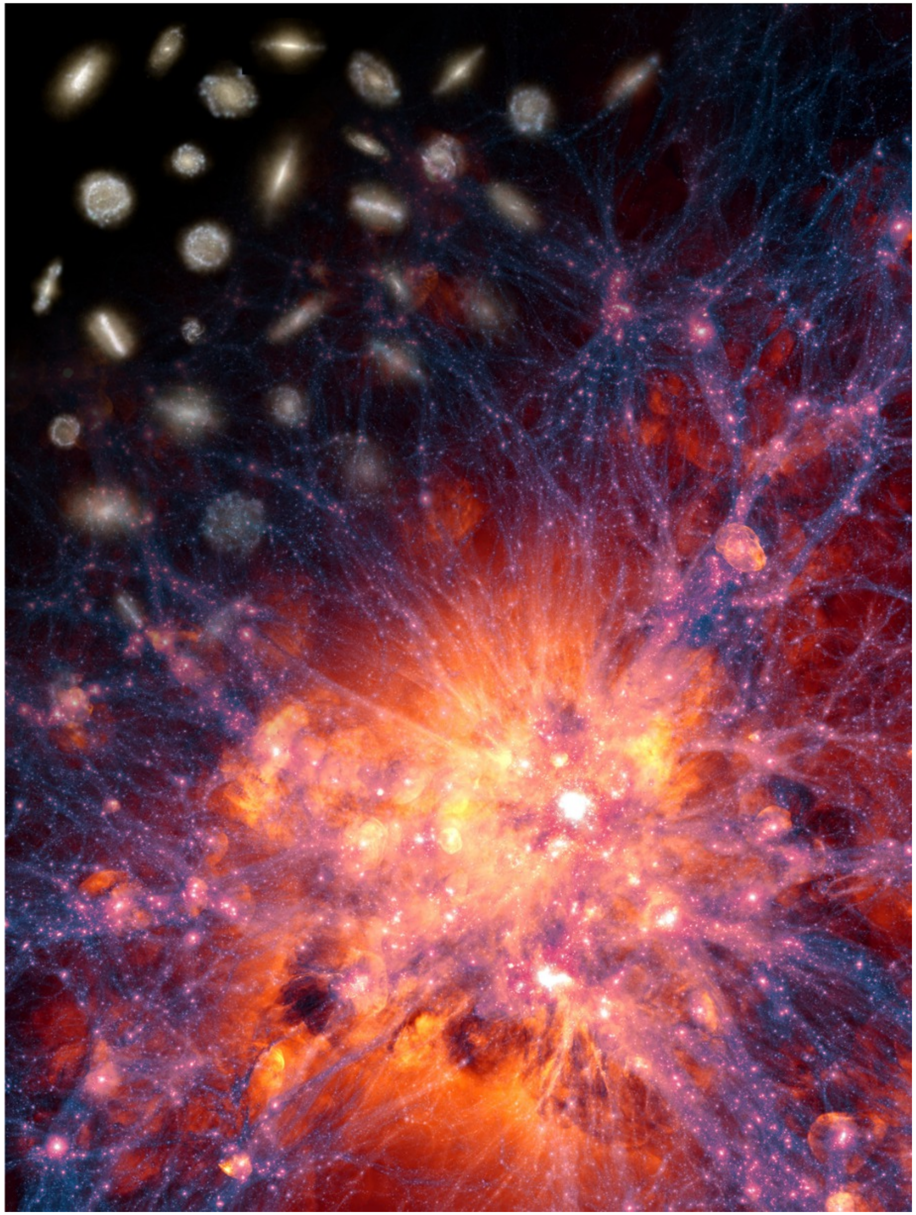

European Research Council
Established by the European Commission

Heidelberg Institute for Theoretical Studies
HITS

Universität Heidelberg

Carving through the Codes
Davos, Switzerland
February 2017

Cosmological simulations bridge 13.7 billion years of (non-linear) evolution

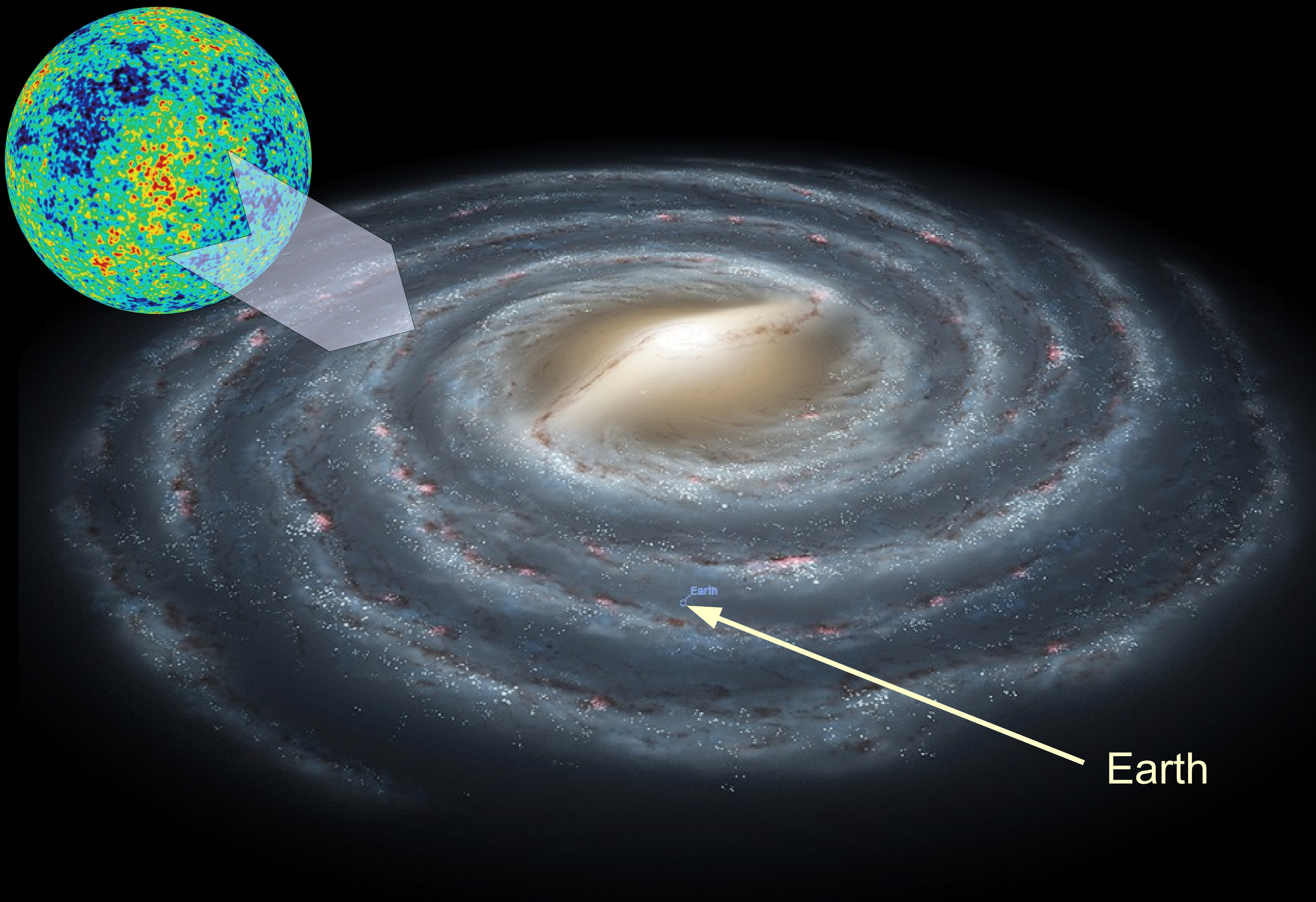

Cosmological N-body simulations accurately predict the emergence of large-scale structure in ΛCDM

COSMIC LARGE-SCALE STRUCTURE IN DARK MATTER

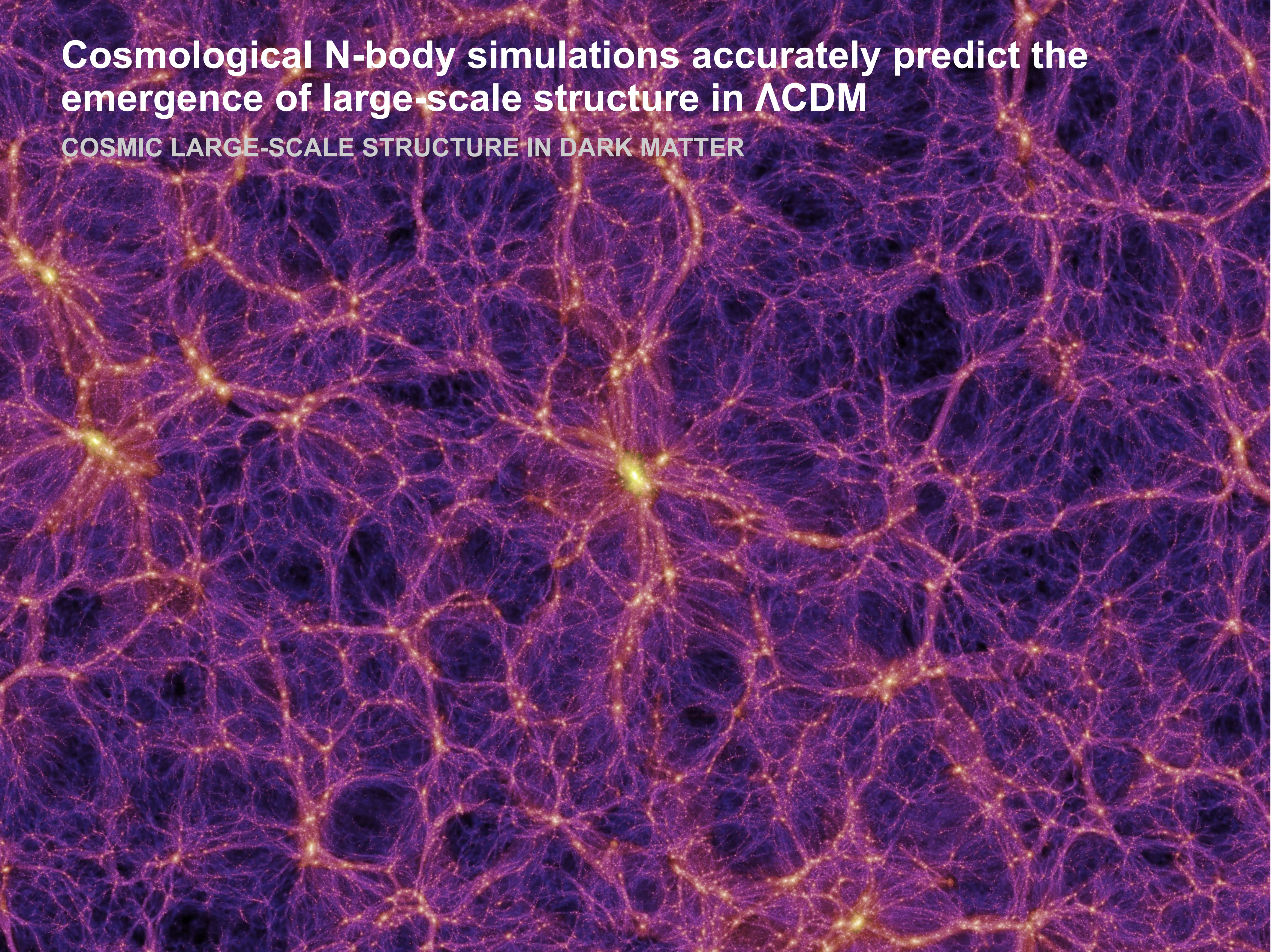

The phase-space structure of galactic halos is very rich and filled with substructures

HALO IN HALOS IN HALOS IN THE AQUARIUS SIMULATIONS

The hierarchy does not appear to be strictly self-similar – we find somewhat fewer substuctures in subhalos than in field halos within the same overdensity.

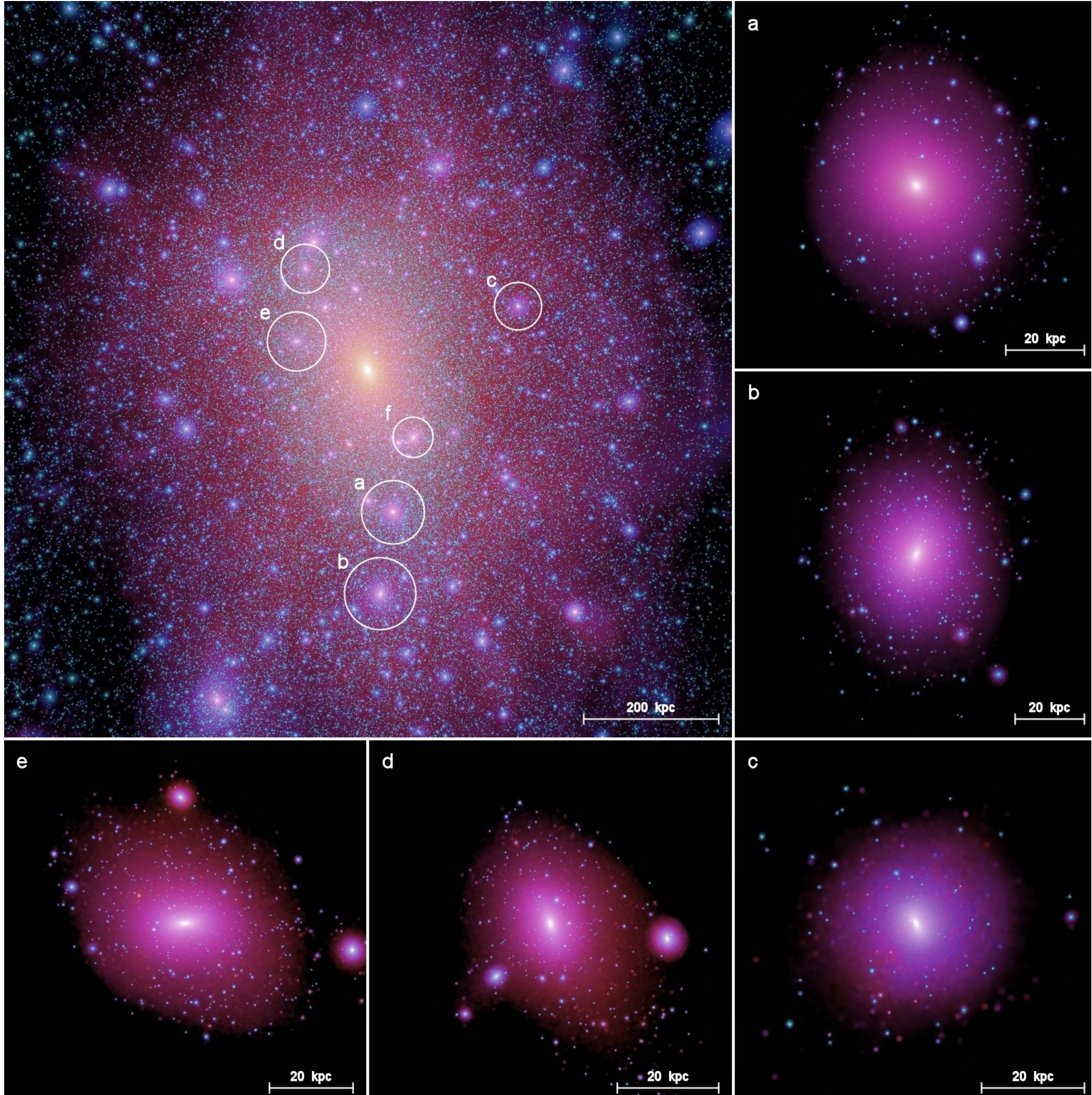

Star formation in the ISM is surprisingly inefficient

THE GAS CONSUMPTION TIMESCALE OF STAR FORMATION

depletion time:

$$t_{\rm dep} \equiv M_{\rm gas}/\dot{M}_*$$

gravitational free-fall time:

$$t_{\rm ff} = \sqrt{\frac{3\pi}{32G\rho}}$$

dimensionless "efficiency" of star formation:

$$\epsilon_{\rm ff} \equiv \frac{t_{\rm ff}}{t_{\rm dep}}$$

observed is:

$$\dot{\Sigma}_\star \simeq \epsilon_{\rm ff} \frac{\Sigma_{\rm H_2}}{t_{\rm ff}}$$

$$\epsilon_{\rm ff} \sim 0.01$$

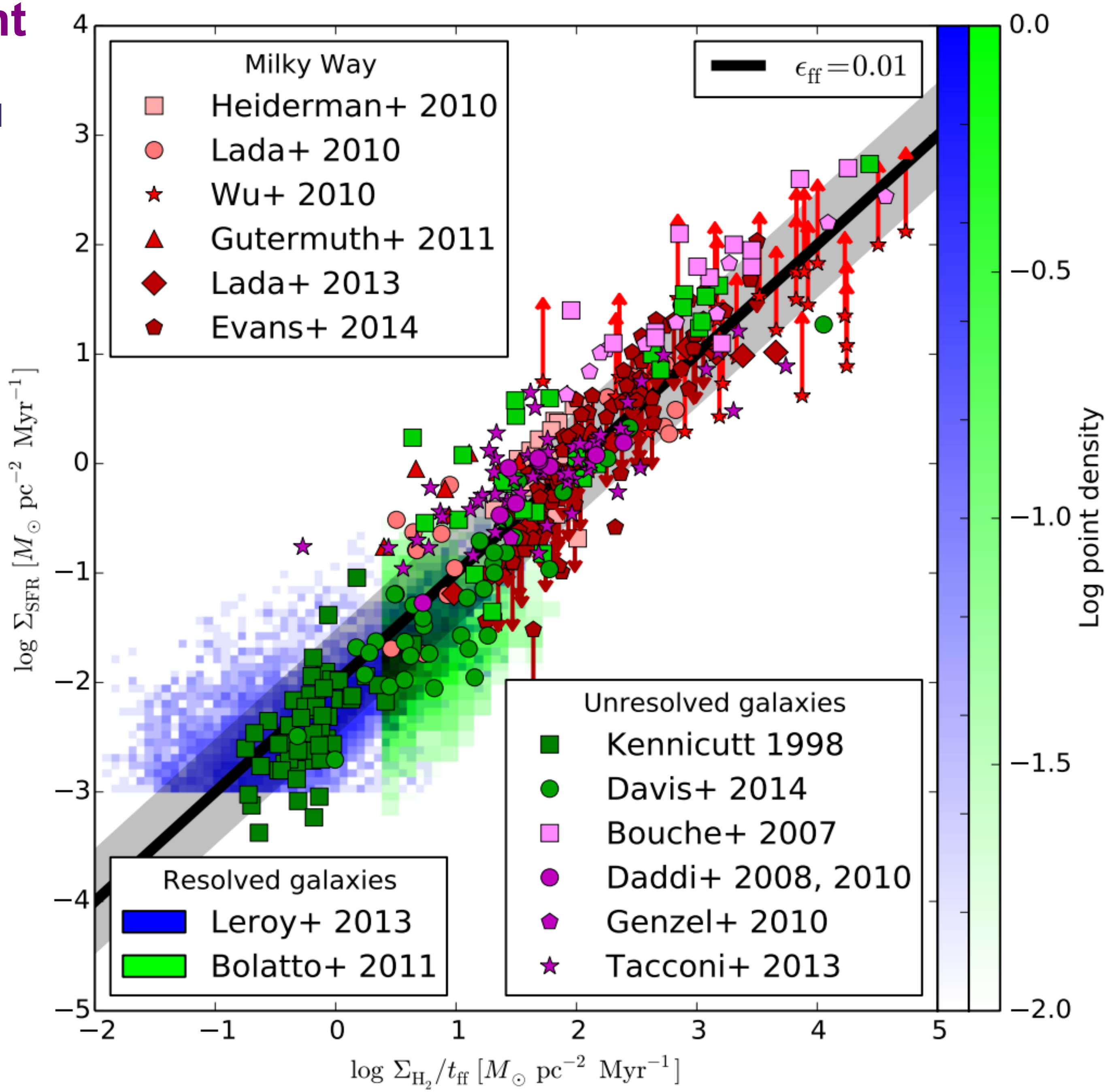

Krumholz et al. (2014)

Abundance matching gives the expected halo mass – stellar mass relation in ΛCDM

MODULATION OF GLOBAL STAR FORMATION EFFICIENCY AS A FUNCTION OF HALO MASS

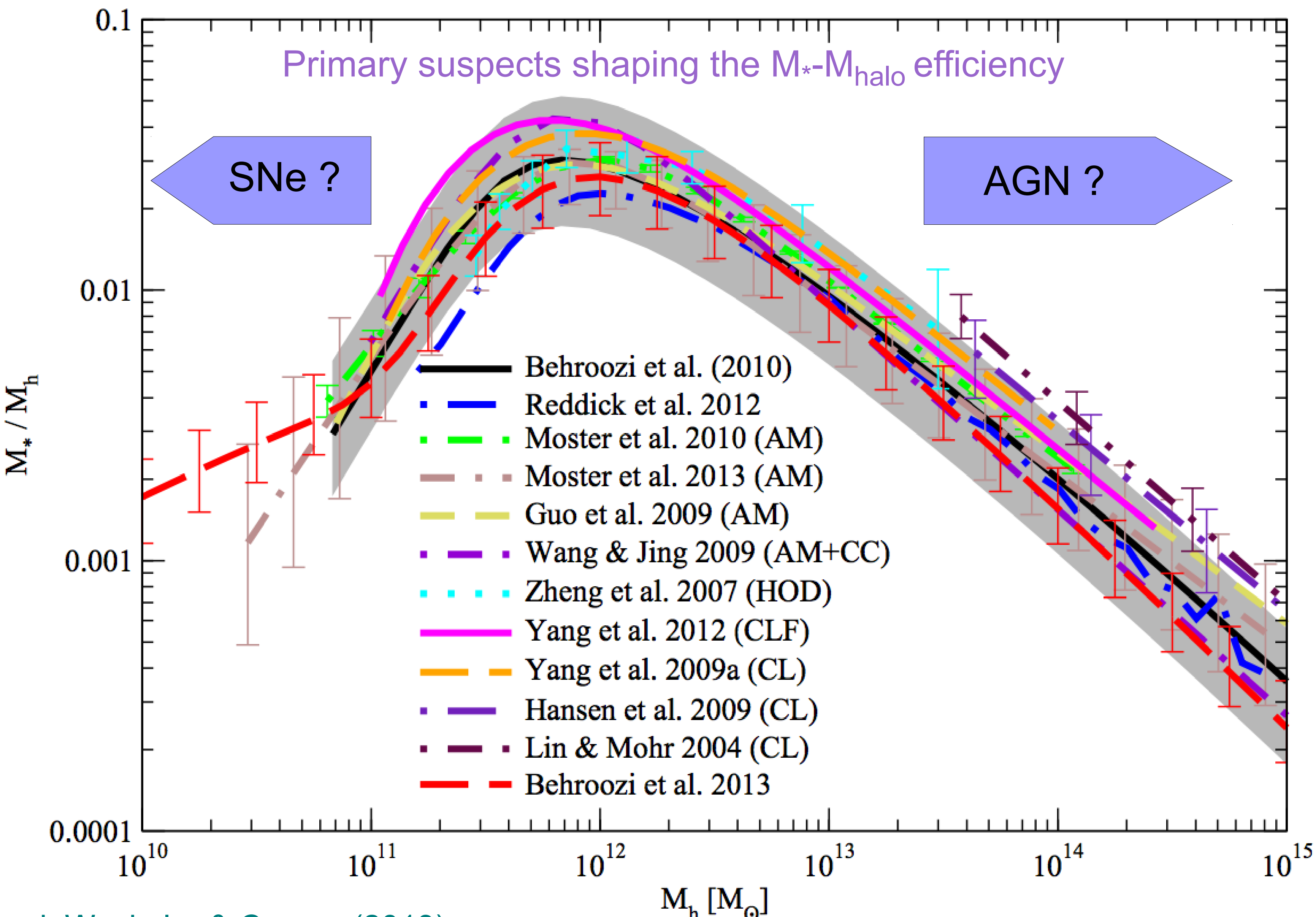

Behroozi, Wechsler & Conroy (2013)

Small scale star formation theories aim to explain why

$$\epsilon_{\rm ff} \sim 0.01$$

Galaxy formation theories need to (additionally) explain why

$$\frac{M_\star}{M_{\rm halo}} \ll \frac{\Omega_b}{\Omega_{\rm tot}}$$

This disconnect is often exploited by galaxy formation studies – they can yield the same result for widely different assumptions about $\varepsilon_{\rm ff}$ on the scale of molecular clouds.

Example:

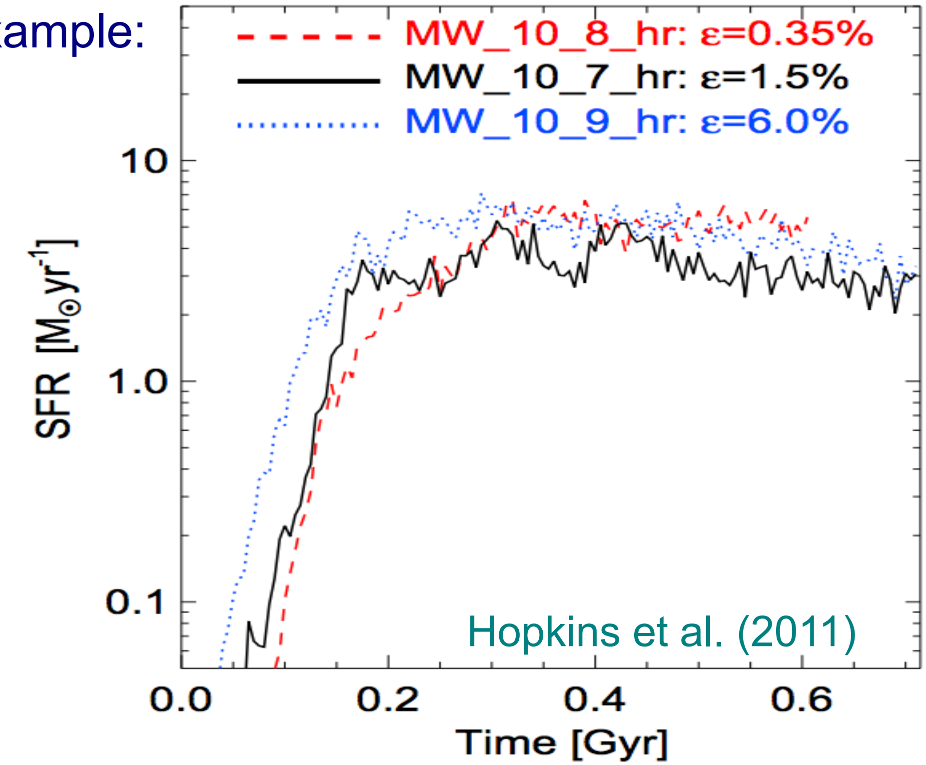

But what physics is responsible for feedback in the first place?

Kepler's Supernova

- **Supernova explosions (energy & momentum input)**

Bubble Nebula

- **Stellar winds**

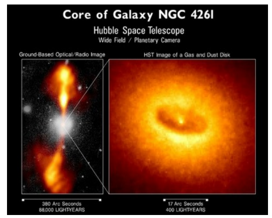

- **AGN activity**

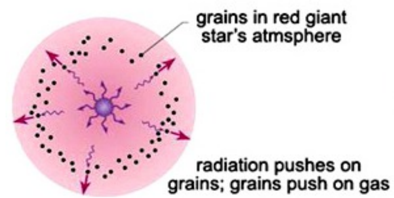

- **Radiation pressure on dust**

Ciardi al. (2003)

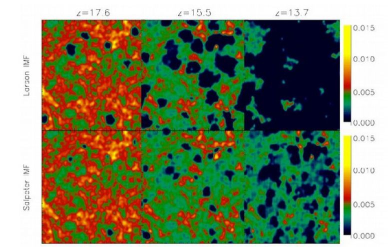

- **Photoionizing UV background and Reionization**

Gneding & Hollon (2012)

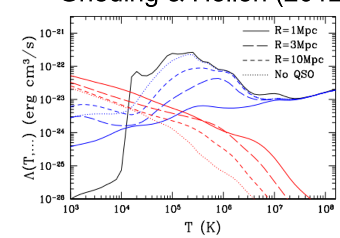

- **Modification of cooling through local UV/X-ray flux**
- **Photoelectric heating**

- **Cosmic ray pressure**

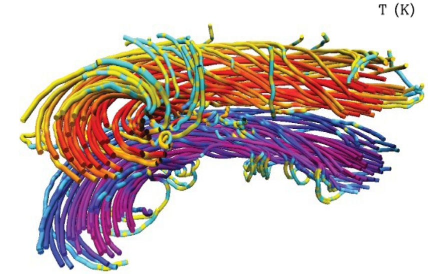

- **Magnetic pressure and MHD turbulence**

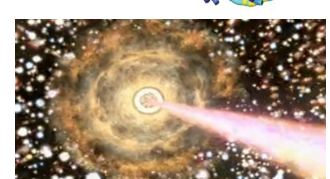

- **TeV-blazar heating of low density gas**

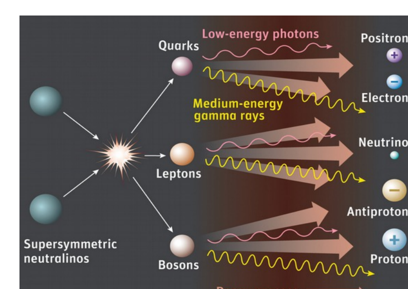

- **Exotic physics (decaying dark matter particles, etc.)**

The **moving-mesh hydrodynamics AREPO** is ideally matched to cosmology

PRINCIPAL ADVANTAGES

- Low numerical viscosity, very low advection errors
- Full adaptivity and manifest Galilean invariance
- Makes larger timesteps possible in supersonic flows
- Crucial accuracy improvement over SPH technique

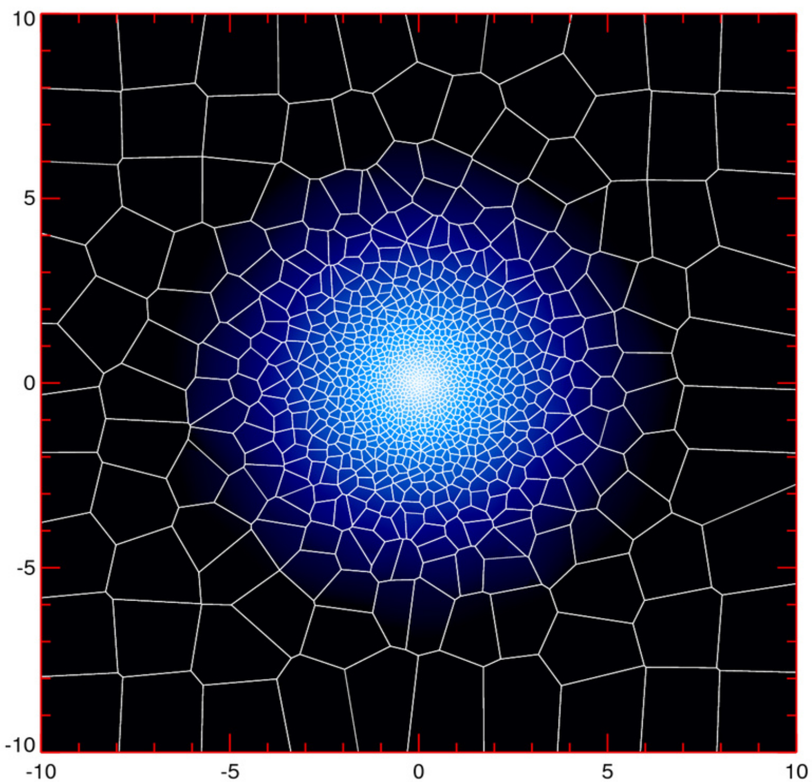

Sketch of flux calculation

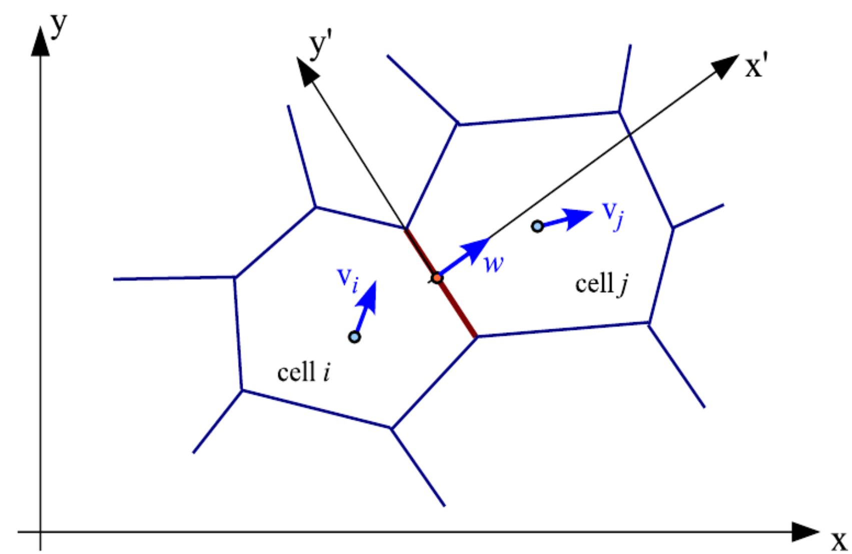

The motion of the mesh generators uniquely determines the motion of all cell boundaries

State left of cell face $\begin{pmatrix} \rho_L \\ \mathbf{v}_L \\ P_L \end{pmatrix}$

State right of cell face $\begin{pmatrix} \rho_R \\ \mathbf{v}_R \\ P_R \end{pmatrix}$

Riemann solver
(in frame of cell face)

$$\rightarrow \begin{pmatrix} \rho \\ \mathbf{v} \\ P \end{pmatrix} \rightarrow \mathbf{F}(\mathbf{U})$$

We have an ideal MHD implementation in AREPO that seems to work well

EQUATIONS AND SOME TESTS

Pakmor, Bauer & Springel (2011)

Pakmor & Springel (2013)

$$\mathbf{U} = \begin{pmatrix} \rho \\ \rho \mathbf{v} \\ \rho e \\ \mathbf{B} \\ \psi \end{pmatrix} \qquad \mathbf{F}(\mathbf{U}) = \begin{pmatrix} \rho \mathbf{v} \\ \rho \mathbf{v}\mathbf{v}^T + p - \mathbf{B}\mathbf{B}^T \\ \rho e \mathbf{v} + p\mathbf{v} - \mathbf{B}\left(\mathbf{v}\cdot\mathbf{B}\right) \\ \mathbf{B}\mathbf{v}^T - \mathbf{v}\mathbf{B}^T + \psi I \\ c_h^2 \mathbf{B} \end{pmatrix}$$

Orszag-Tang vortex test

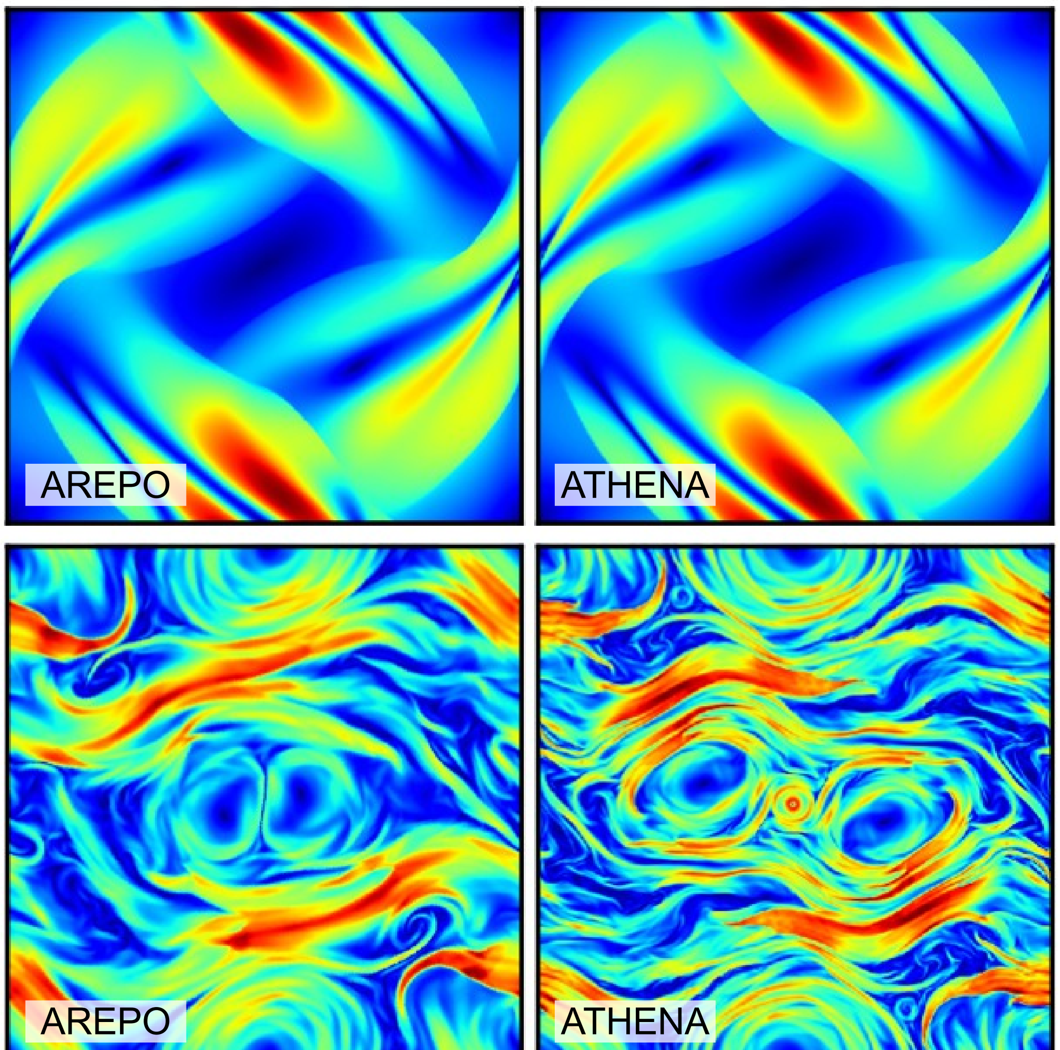

- 8-wave Powell scheme for divergence cleaning
- Approximate HLLD Riemann solver

Loss of magnetic energy in moving field loop

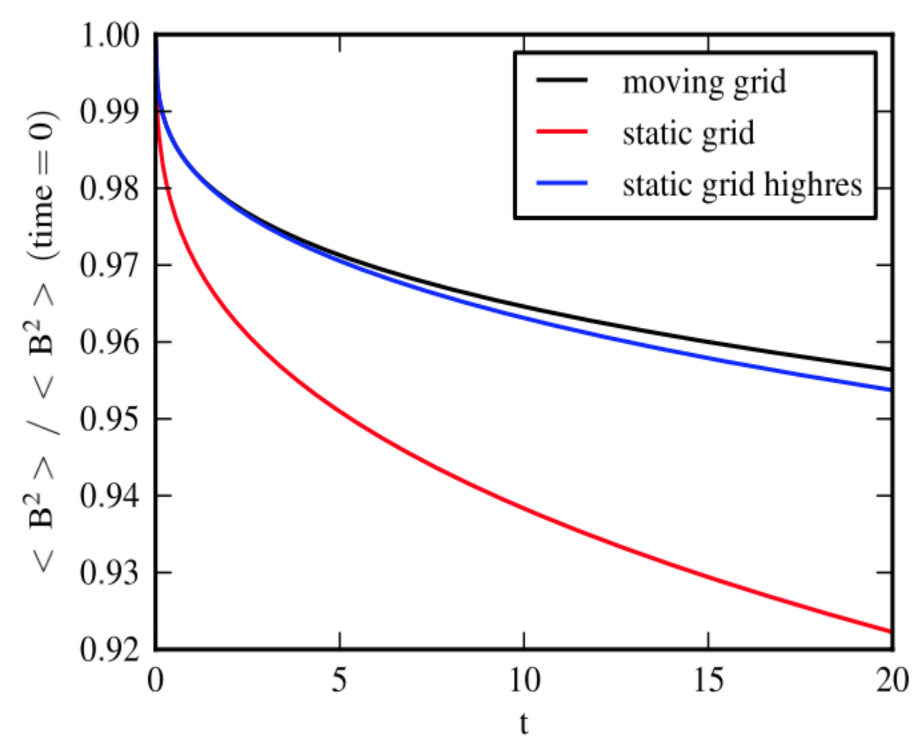

“Auriga”
Milky Way-like
galaxies

Results from AURIGA

30 HIGH-RESOLUTION MILKY WAY-SIZED HALOS

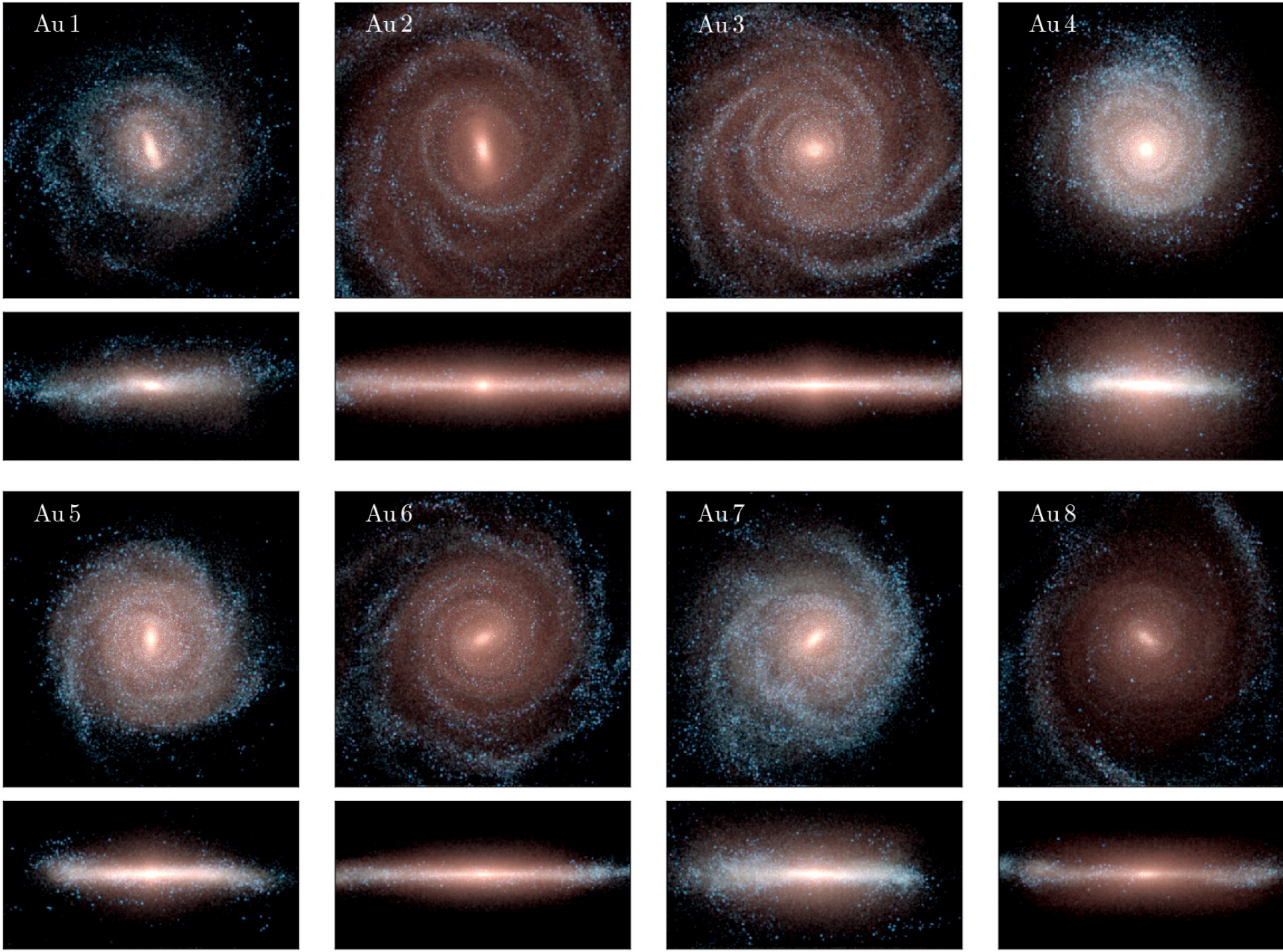

The disk sizes match observational constraints

EXPONENTIAL DISK SCALE LENGTHS AND HALF-MASS RADII AS A FUNCTION OF STELLAR MASS

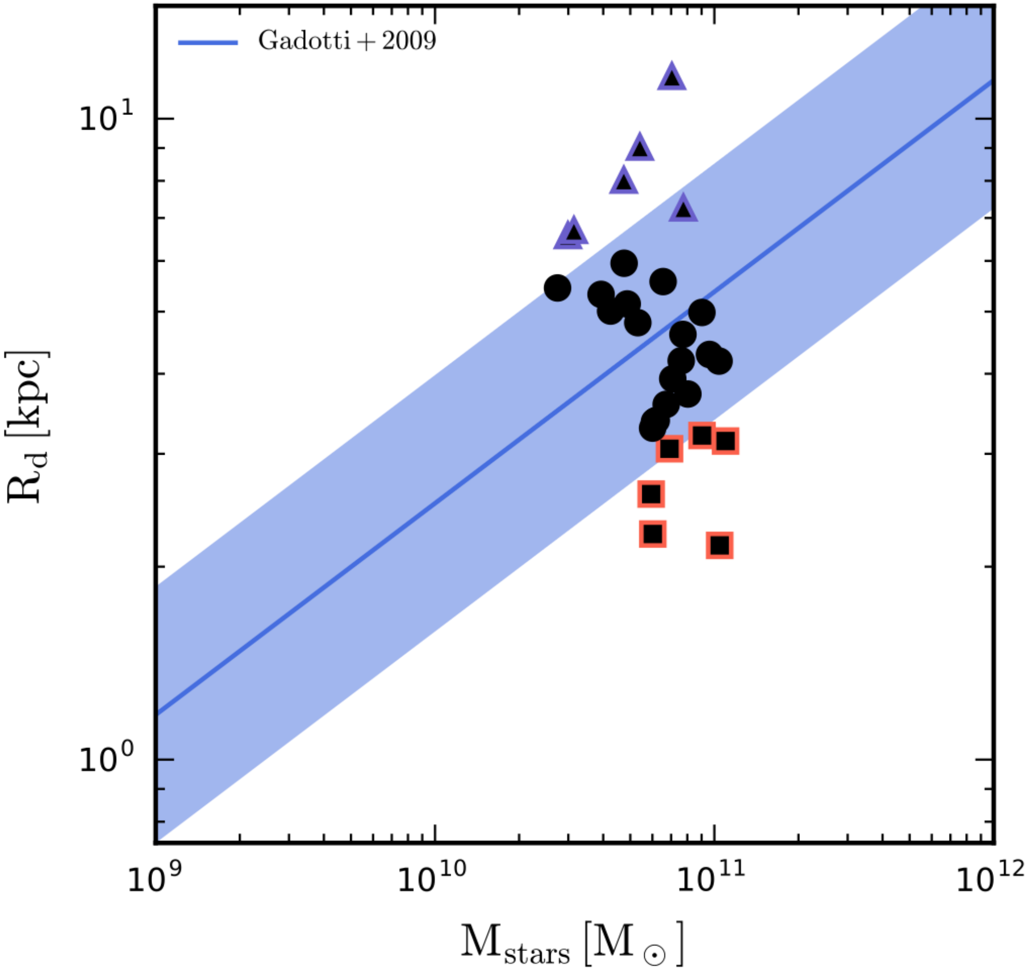

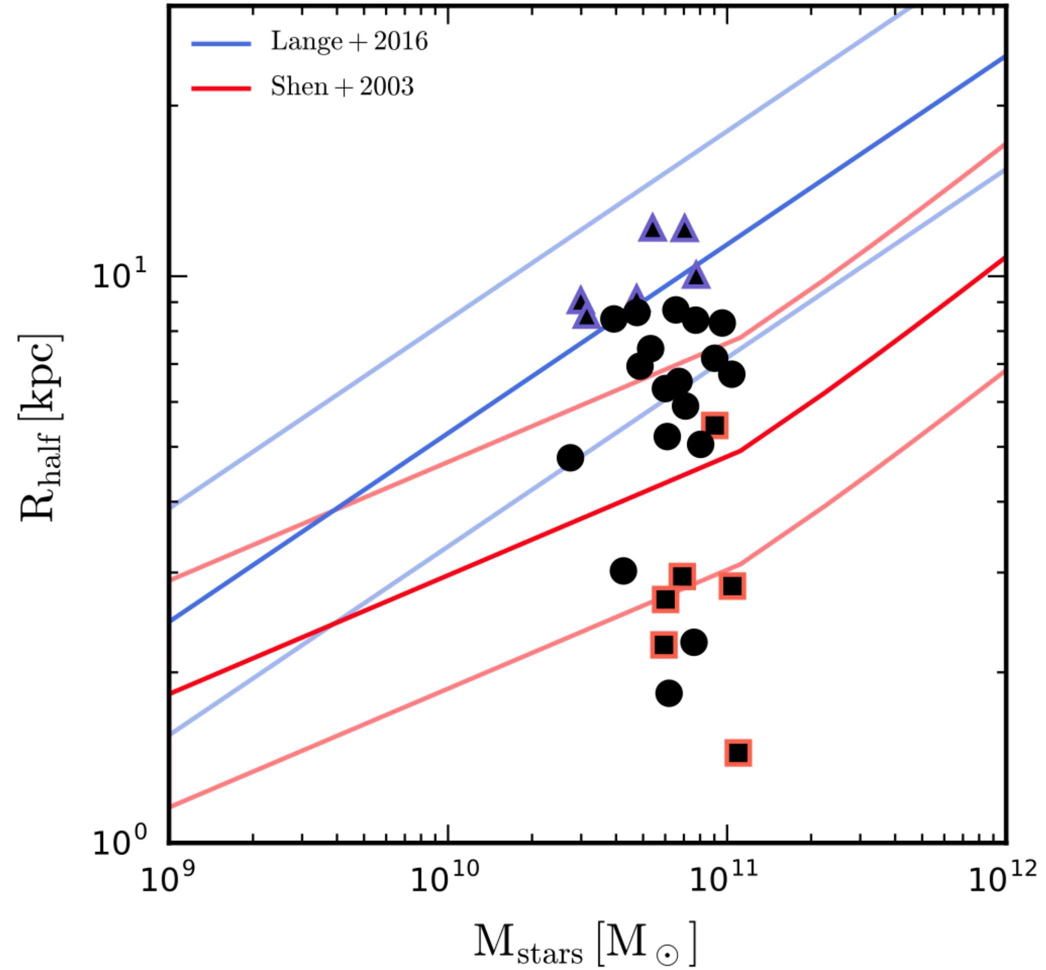

Grand et al. (2016)

Disk dominated systems with small bulges are formed

ORBITAL CIRCULARITY DISTRIBUTION

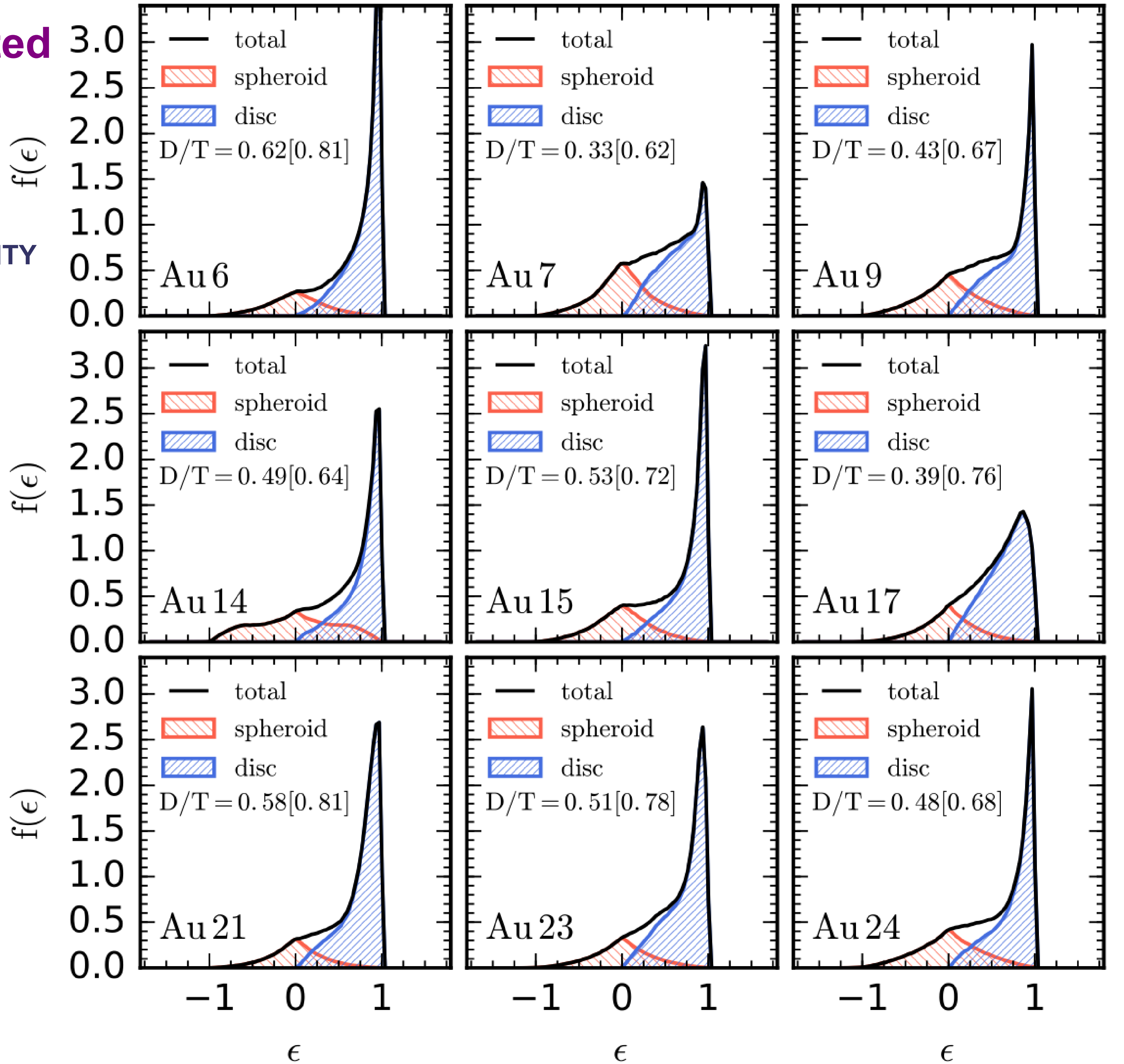

Grand et al. (2016)

The simulations are late-type, blue cloud star forming galaxies

COLORS AND STAR FPRMATION RATES AS A FUNCTION OF MAGNITUDE OR STELLAR MASS

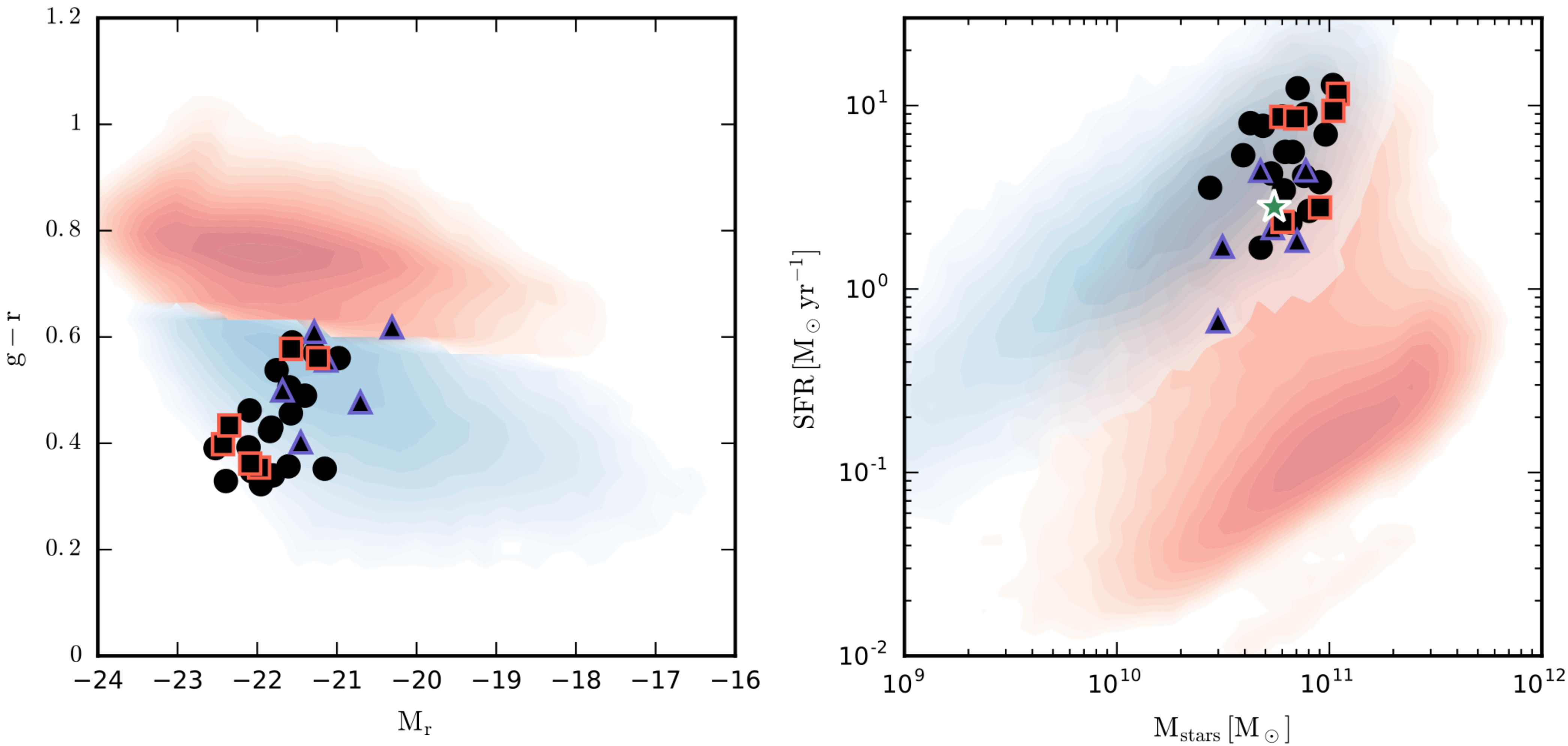

Grand et al. (2016)

Black hole growth influences disk sizes

BLACK HOLE GROWTH BETWEEN Z=1 AND Z=0 CORRELATED WITH DISK SCALE LENGTHS

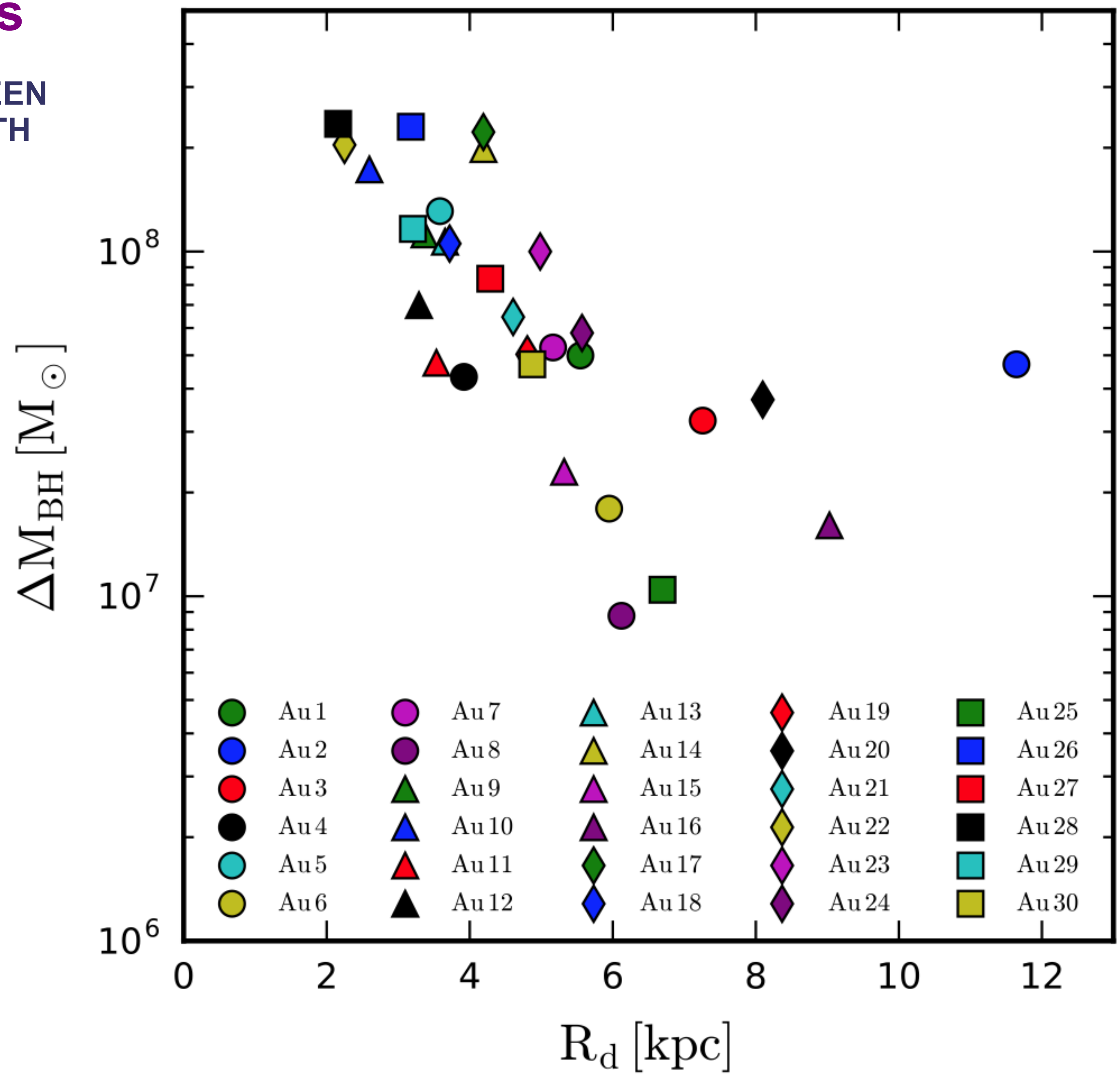

Grand et al. (2016)

The models converge reasonable well, ***for fixed model parameters***

SURFACE BRIGHTNESS, ORBITAL CIRCULARITY AND VERTICAL DISC SCALE HEIGHT COMPARED AT VERY DIFFERENT NUMERICAL RESOLUTION

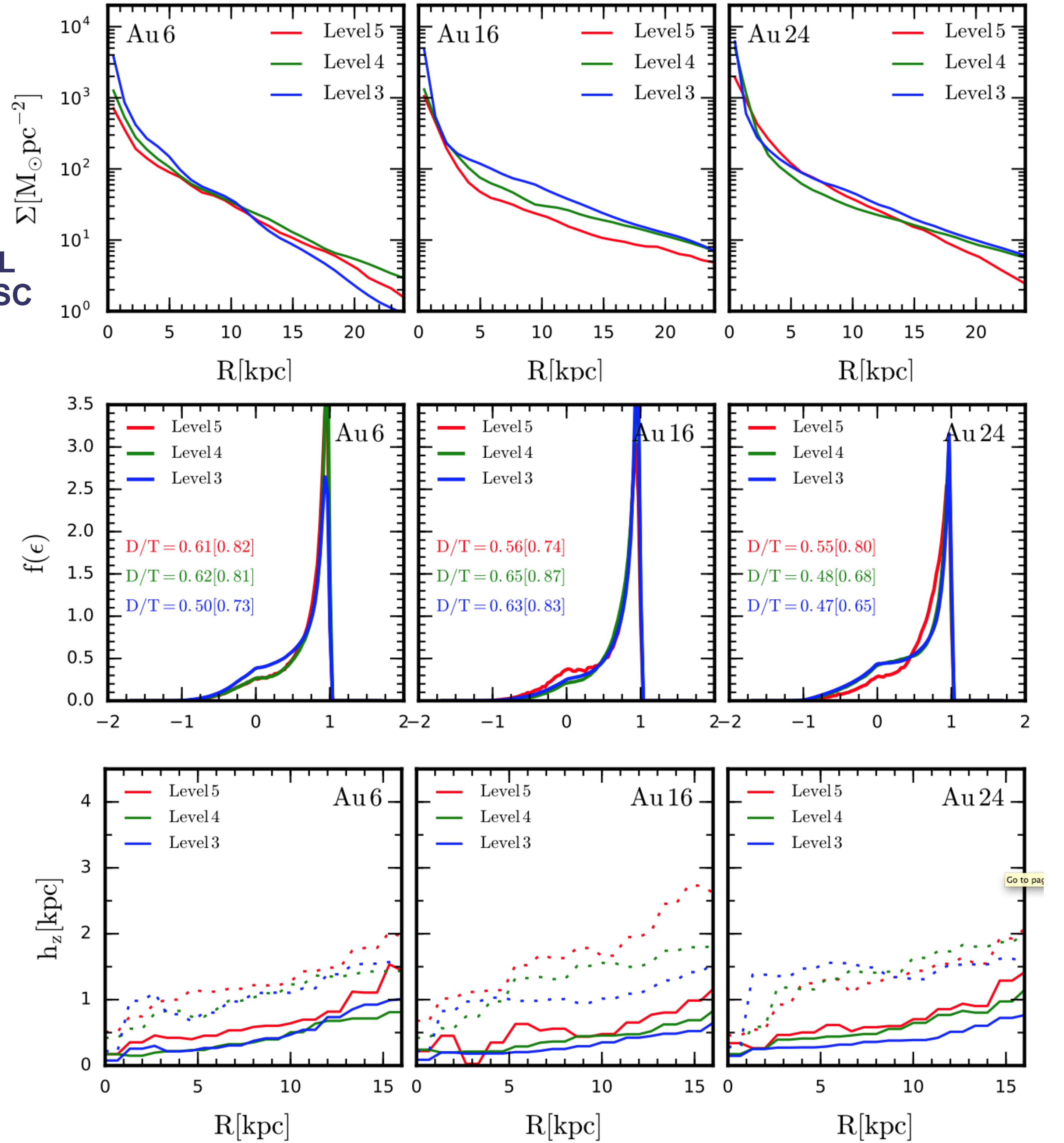

Grand et al. (2016)

The morphology of neutral gas is very different from the stars

HI PROJECTIONS OF AURIGA GALAXIES

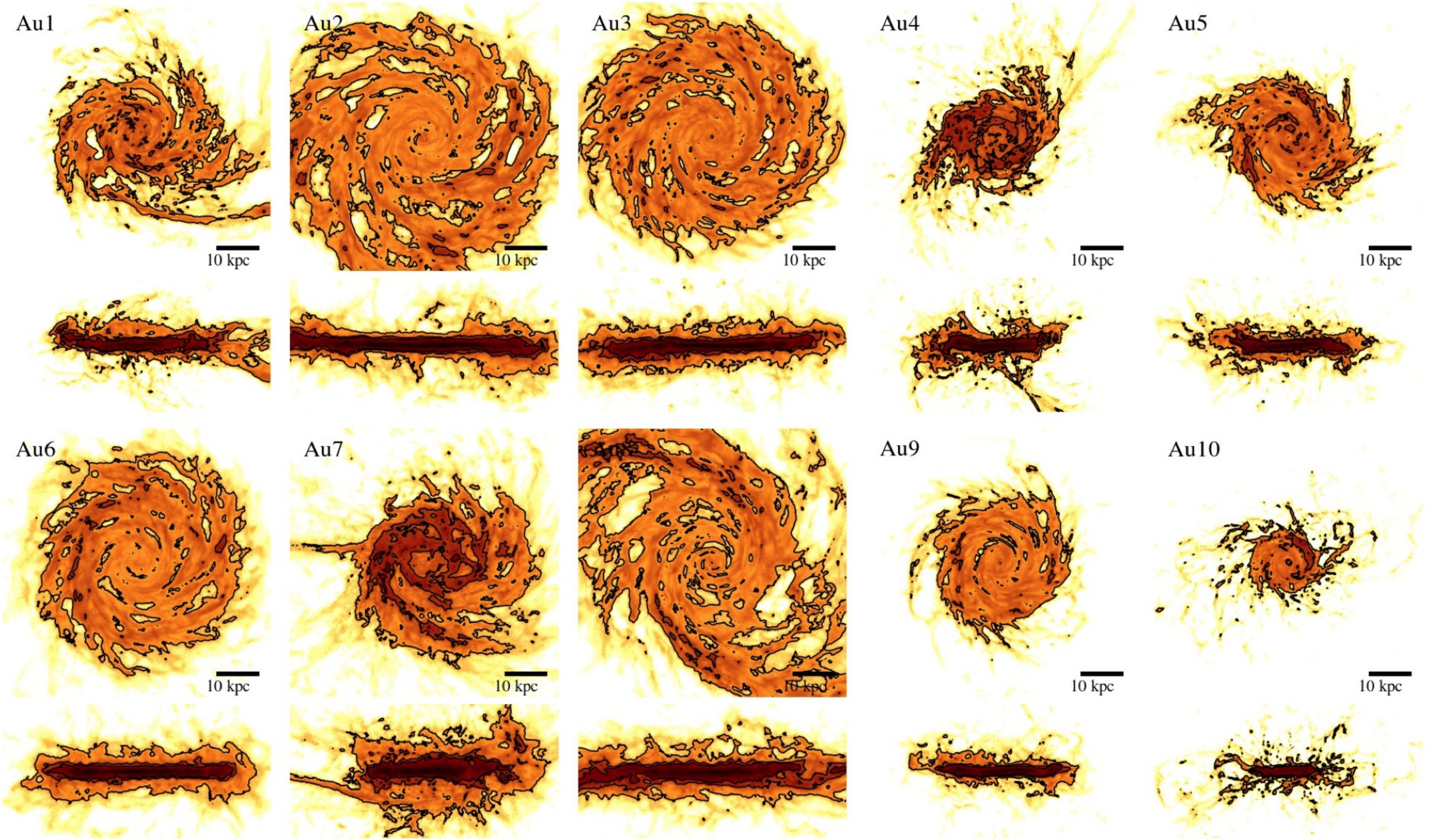

Marinacci et al. (2016)

HI properties are in broad agreement with observational constraints

HI SURFACE DENSITIES, HI MASSES, AND TOTAL GAS FRACTIONS OF SIMULATED DISKS COMARED TO DATA

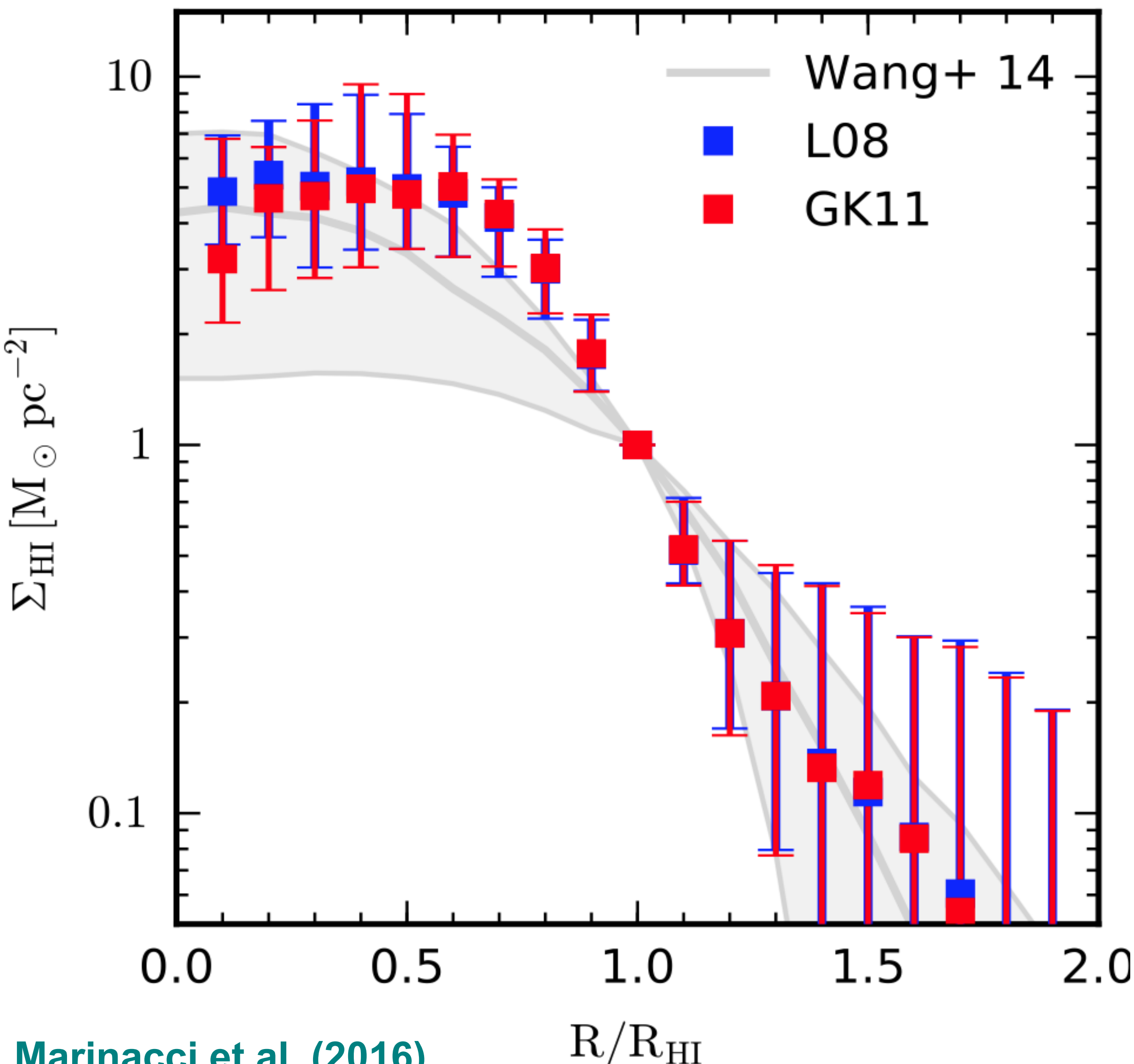

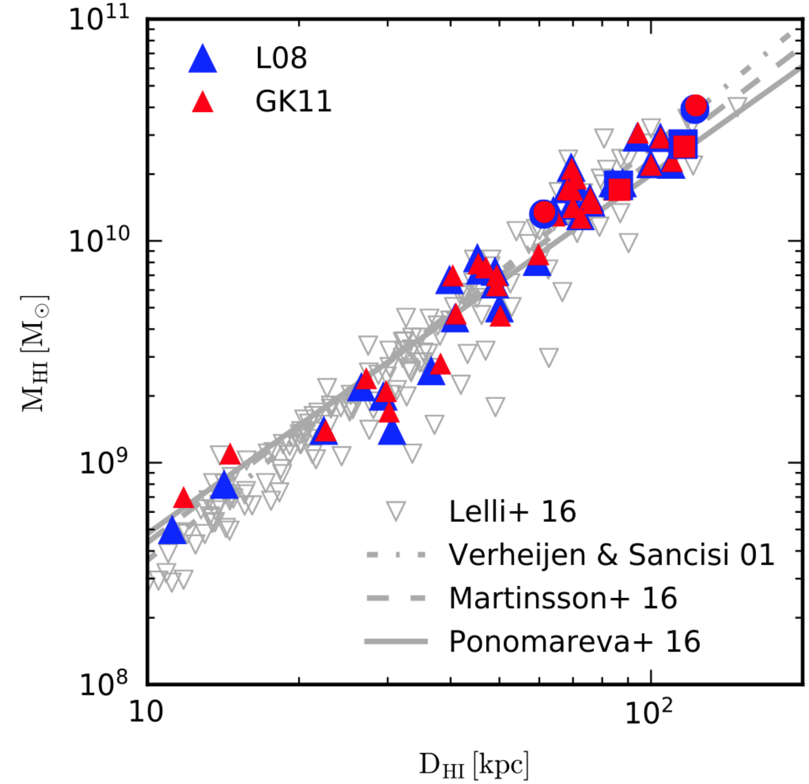

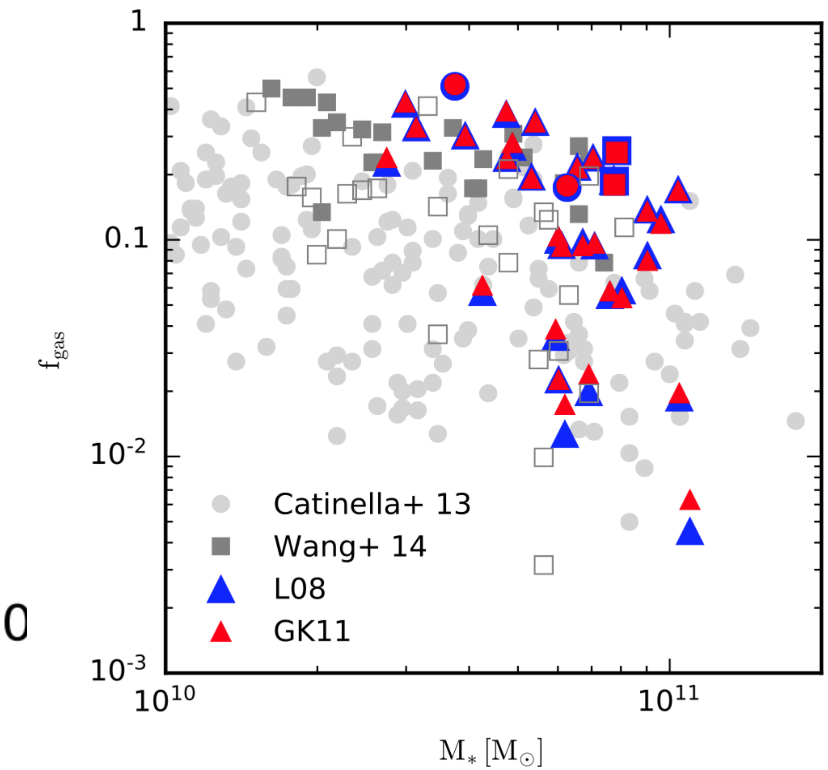

Marinacci et al. (2016)

Magnetic fields

MHD simulations of galaxy formation predict the amplification of primordial fields in halos and galaxies

MAGNETIC FIELD STRENGTH IN A SMALL REGION OF ILLUSTRIS-TNG

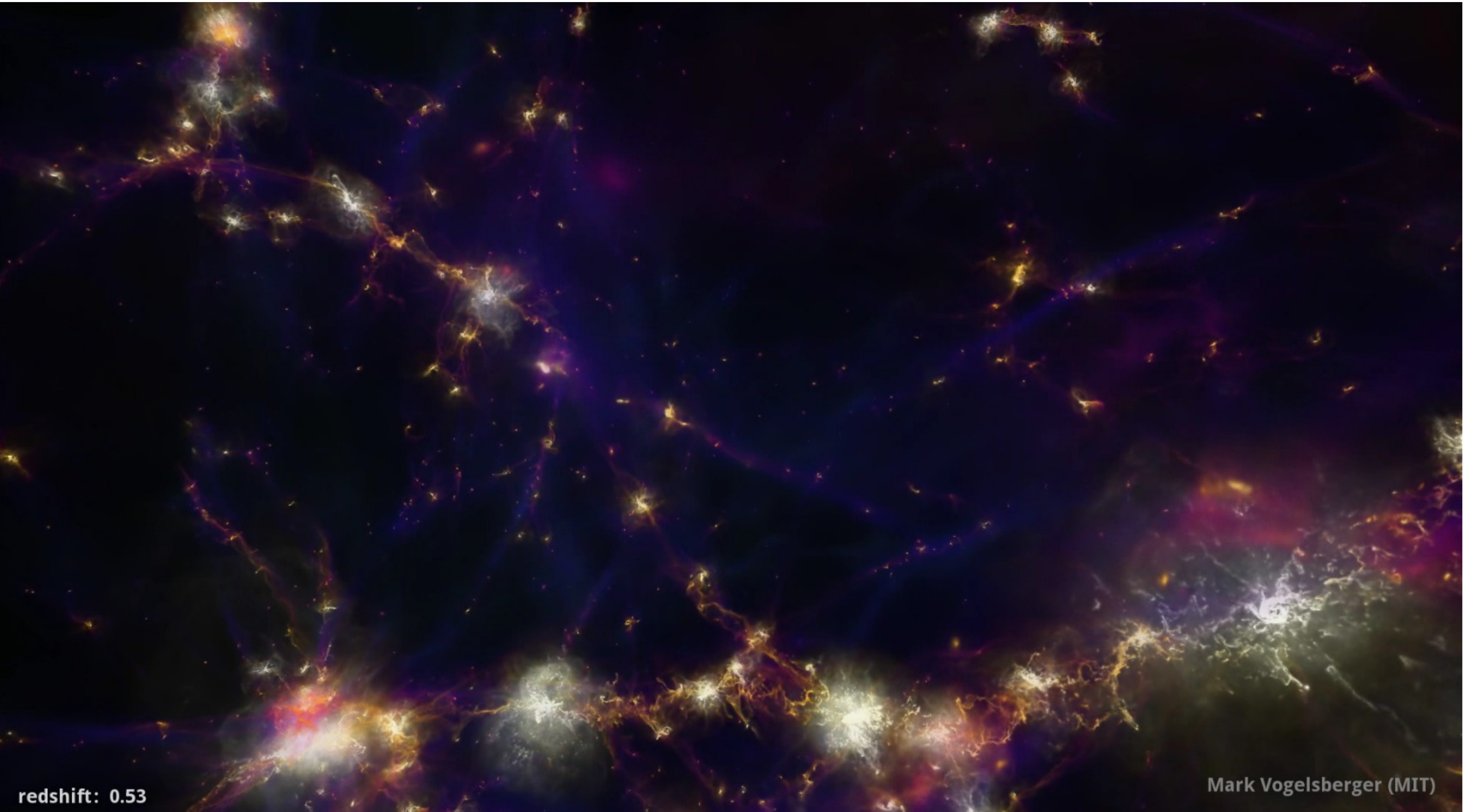

The non-radiative and full physics simulations differ strongly in the B-field amplification in the dense gas

REDSHIFT EVOLUTON OF THE B-FIELD STRENGTH VS BARYON OVERDENSITY Marinacci et al. (2015)

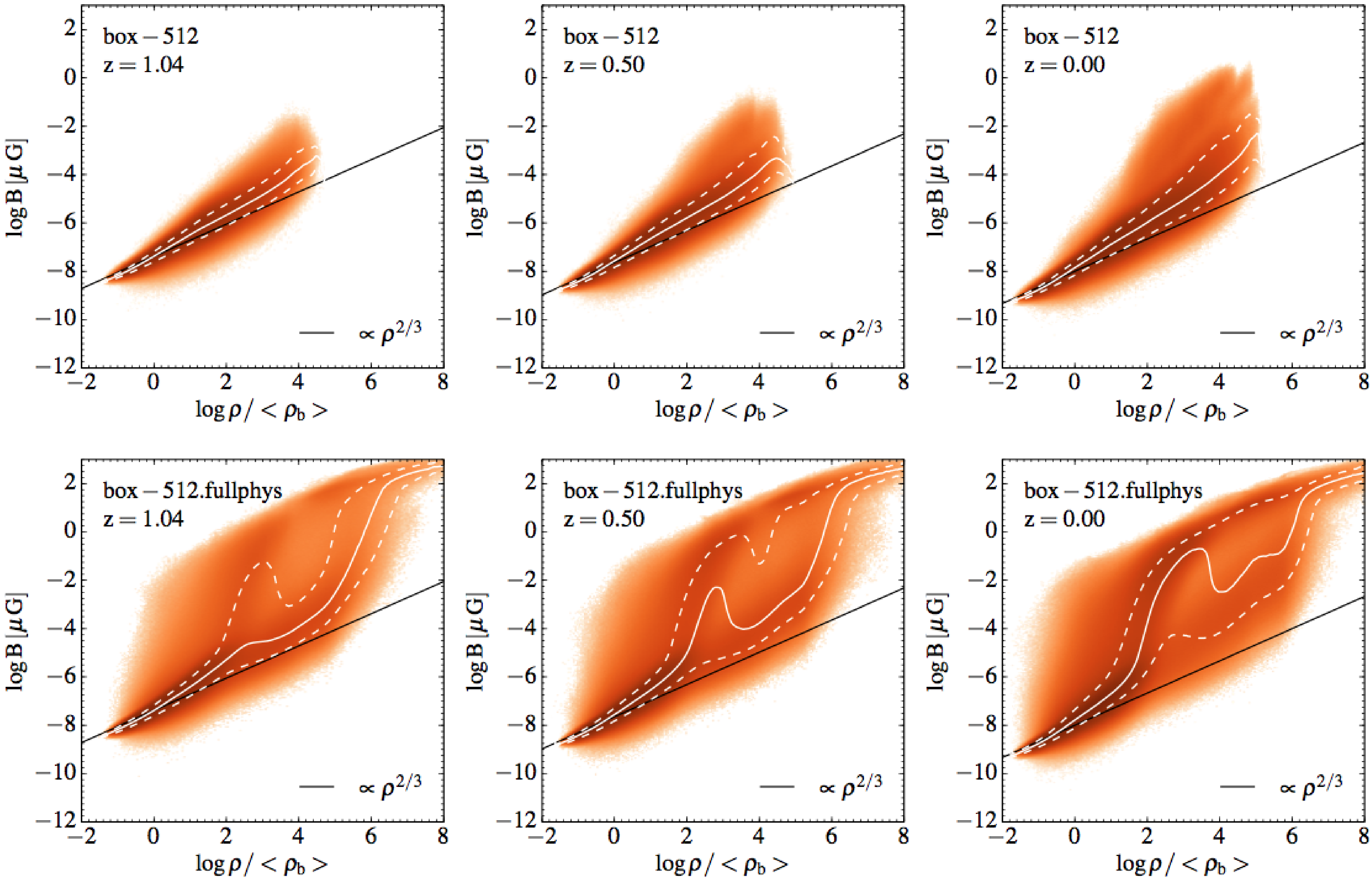

The low redshift volume-weighted B-field strength in the full physics simulation is fairly independent of the seed field

EVOLUTON OF THE VOLUME-WEIGHTE B-FIELD FOR DIFFERENT SEED FIELDS AND PHYSICS

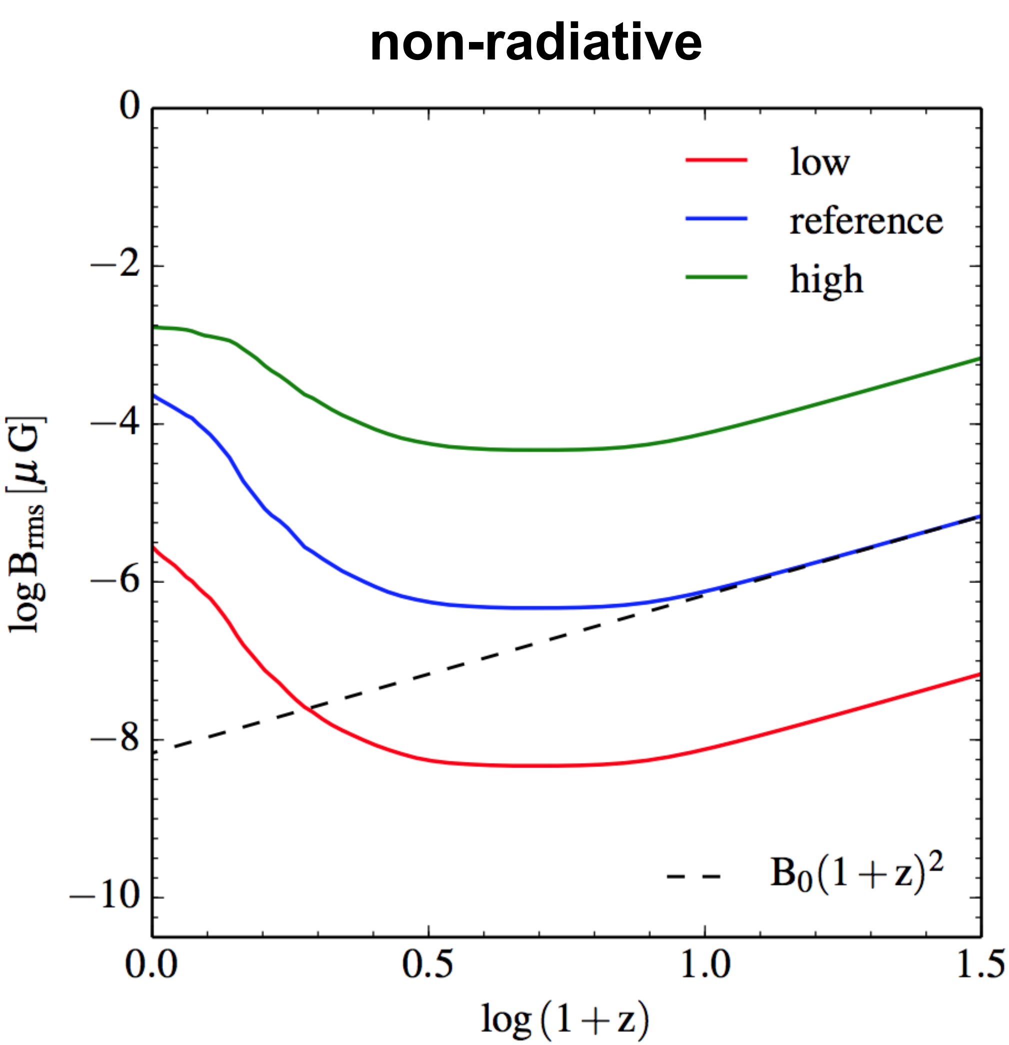

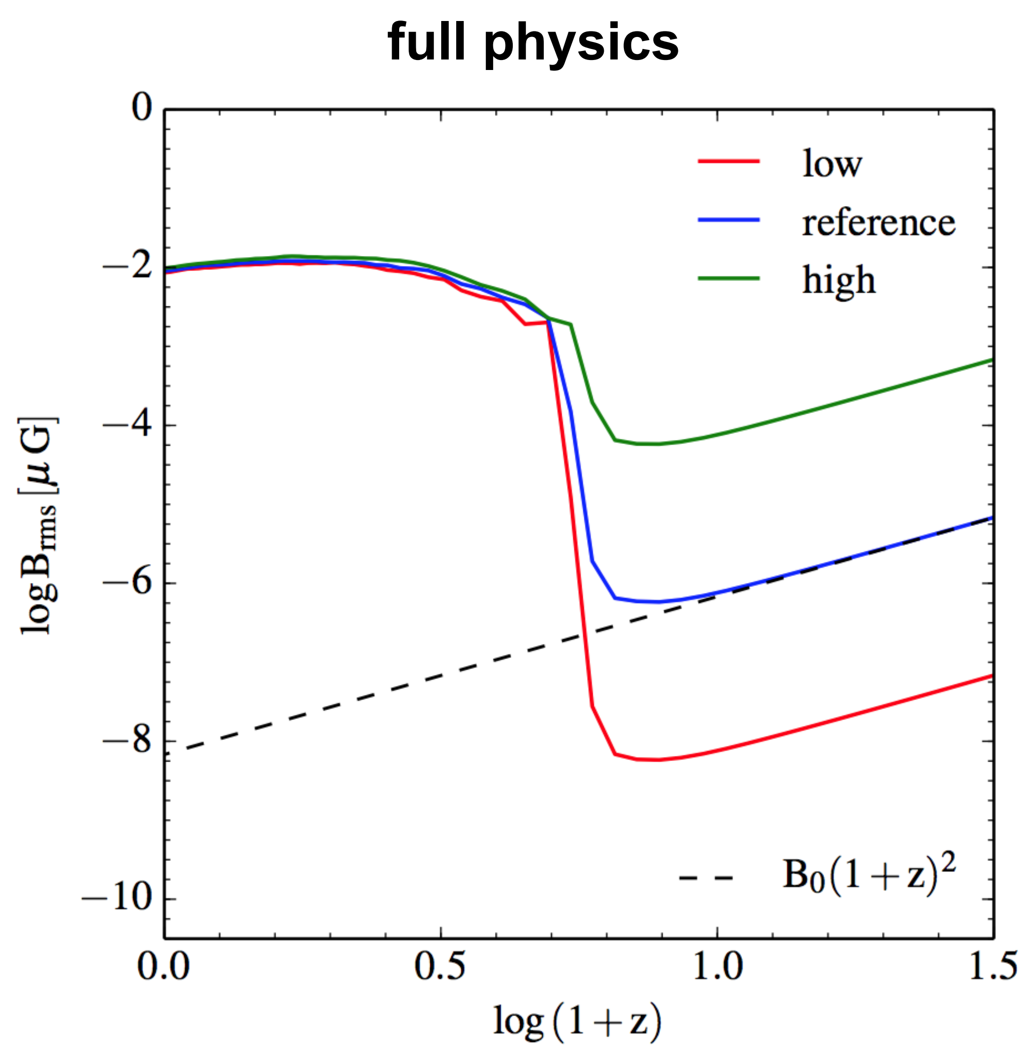

Marinacci et al. (2015)

In filaments, memory of the initial field geometry is still kept, and this affects also the amplification

FIELD DISTRIBUTION IN TWO IDENTICAL SIMULATIONS WHERE THE INITIAL ORIENTATION OF THE B-FIELD WAS CHANGED

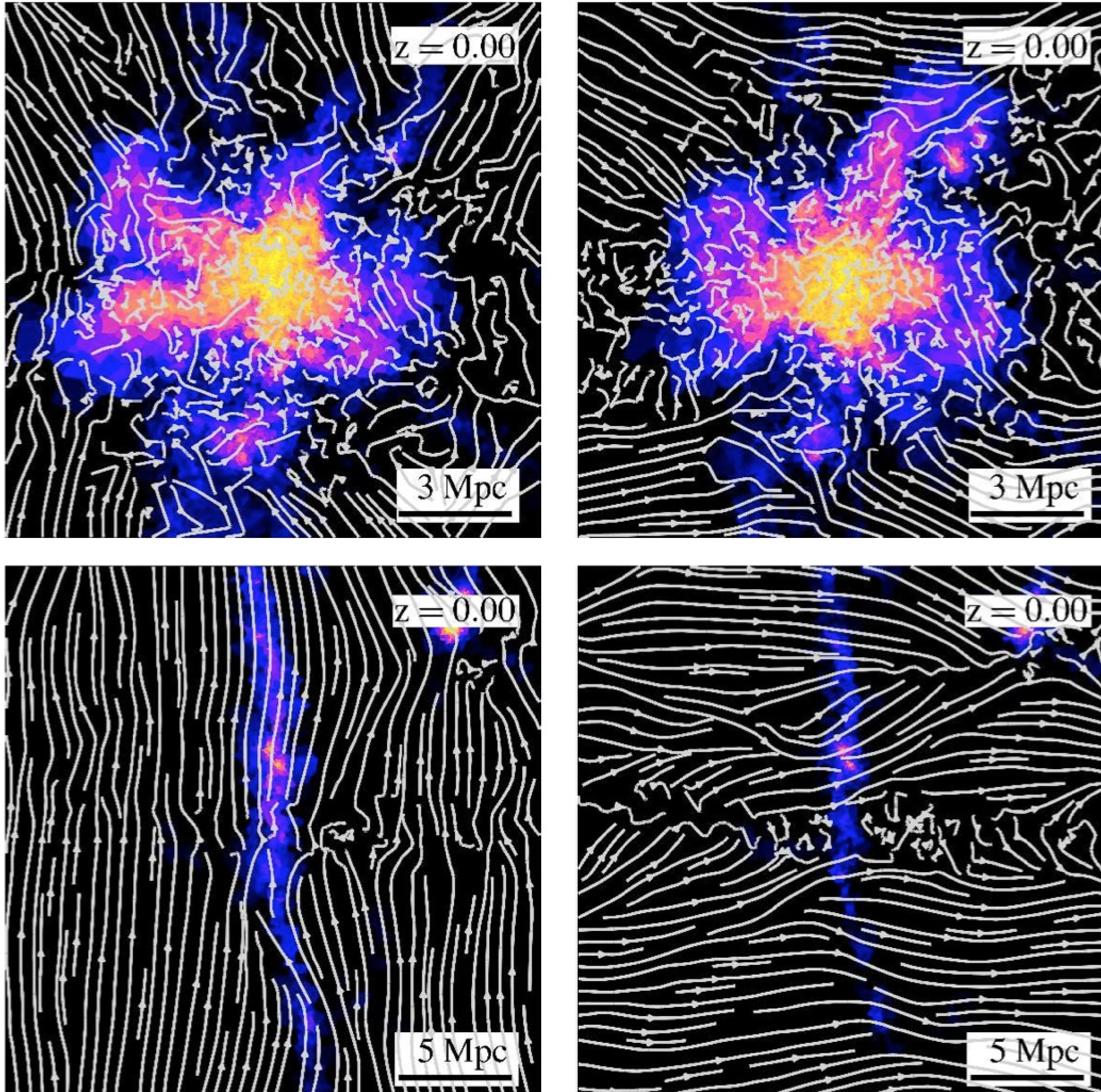

Marinacci et al. (2015)

The predicted present-day B-field is largely toroidal

MAGNETIC FIELD IN THE DISK AT REDSHIFT Z=0

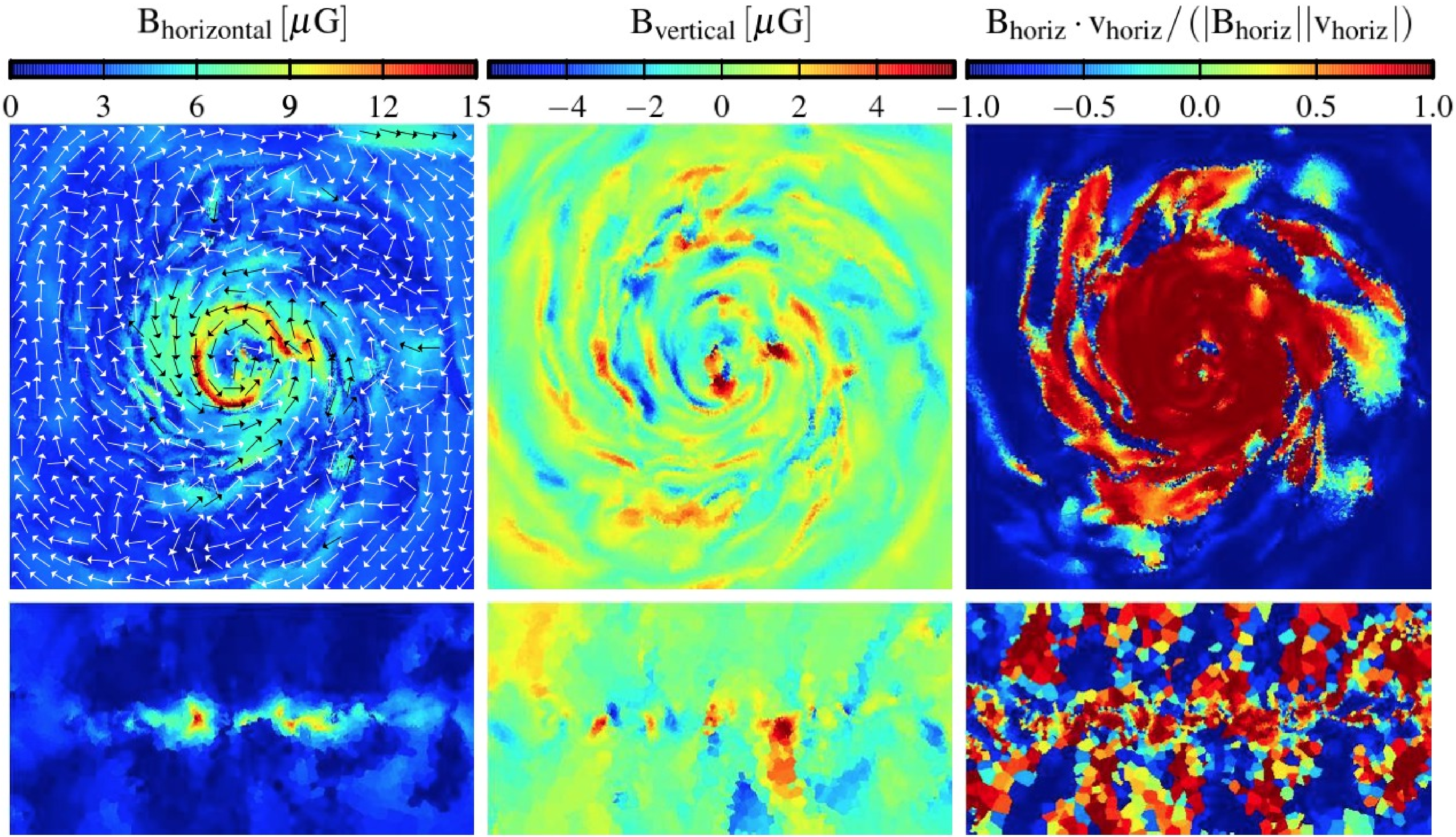

The small-scale dynamo is active at very high redshift

EVOLUTION OF THE VOLUME-WEIGHTED RMS B-FIELD STRENGTH FOR DIFFERENT SEED FIELDS

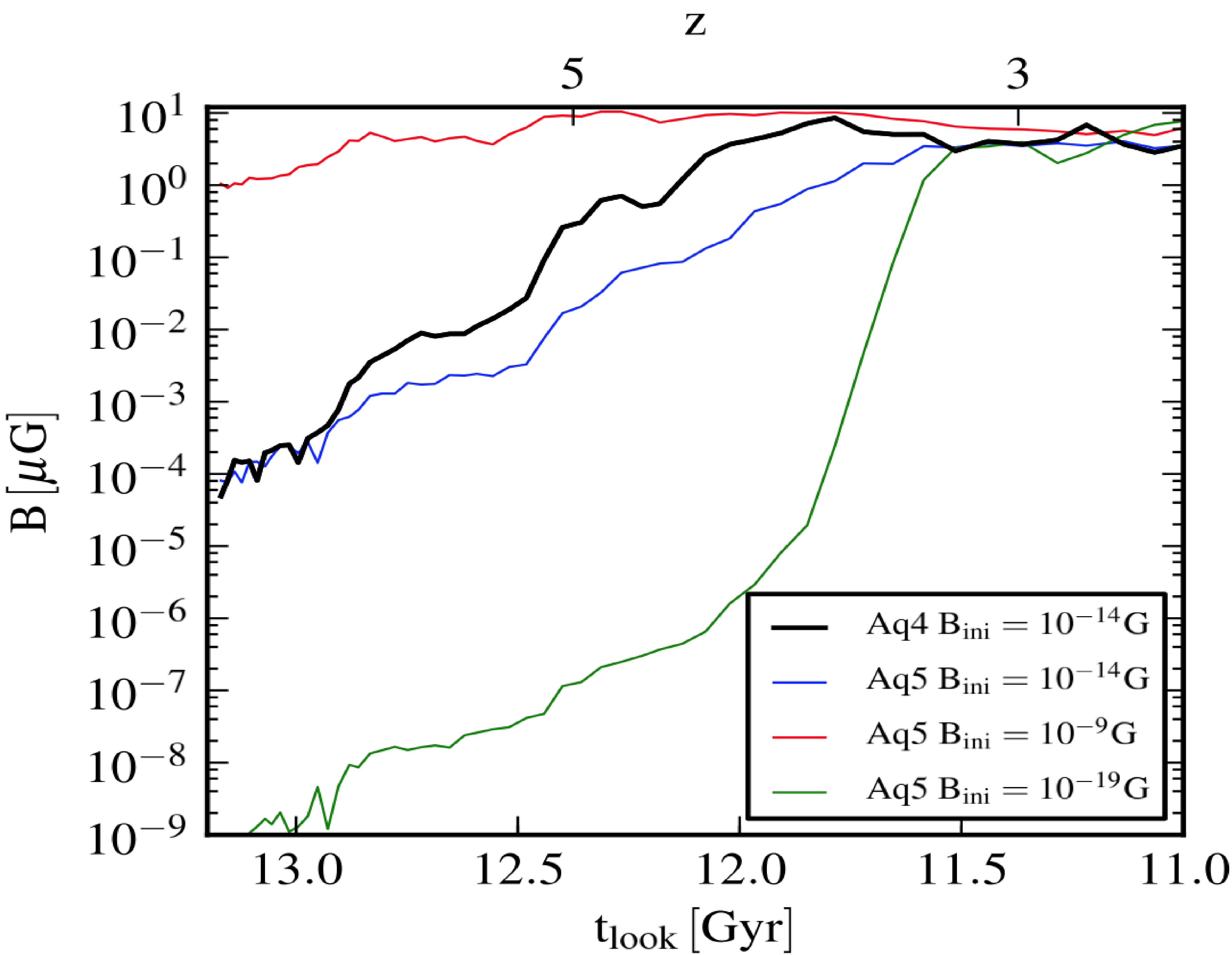

Little residual amplification happens in the disks themselves once the small-scale dynamo has saturated

TIME EVOLUTION OF THE B-FIELD AVERAGED OVER ALL AURIGA GALAXIES

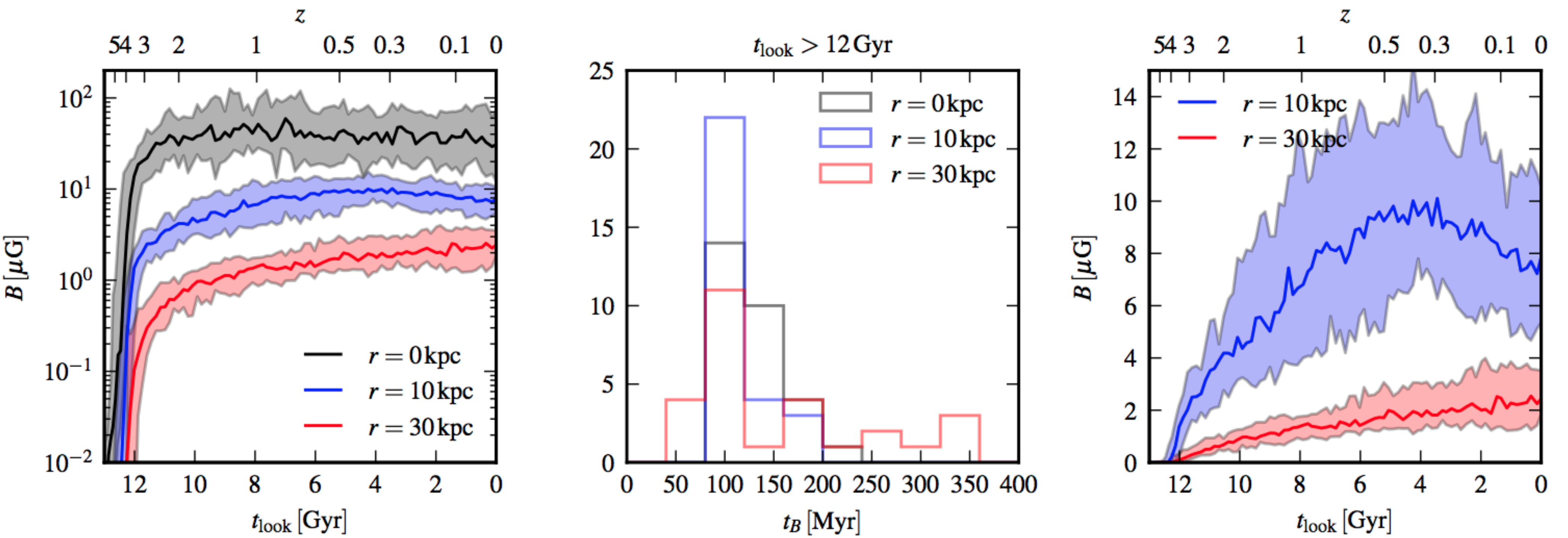

Pakmor et al. (2017)

The magnetic field shows double power-law exponential profiles in the radial direction

PROJECTED B-FIELD ENERGY DENSITY AND RADIAL MAGNETIC PROFILES

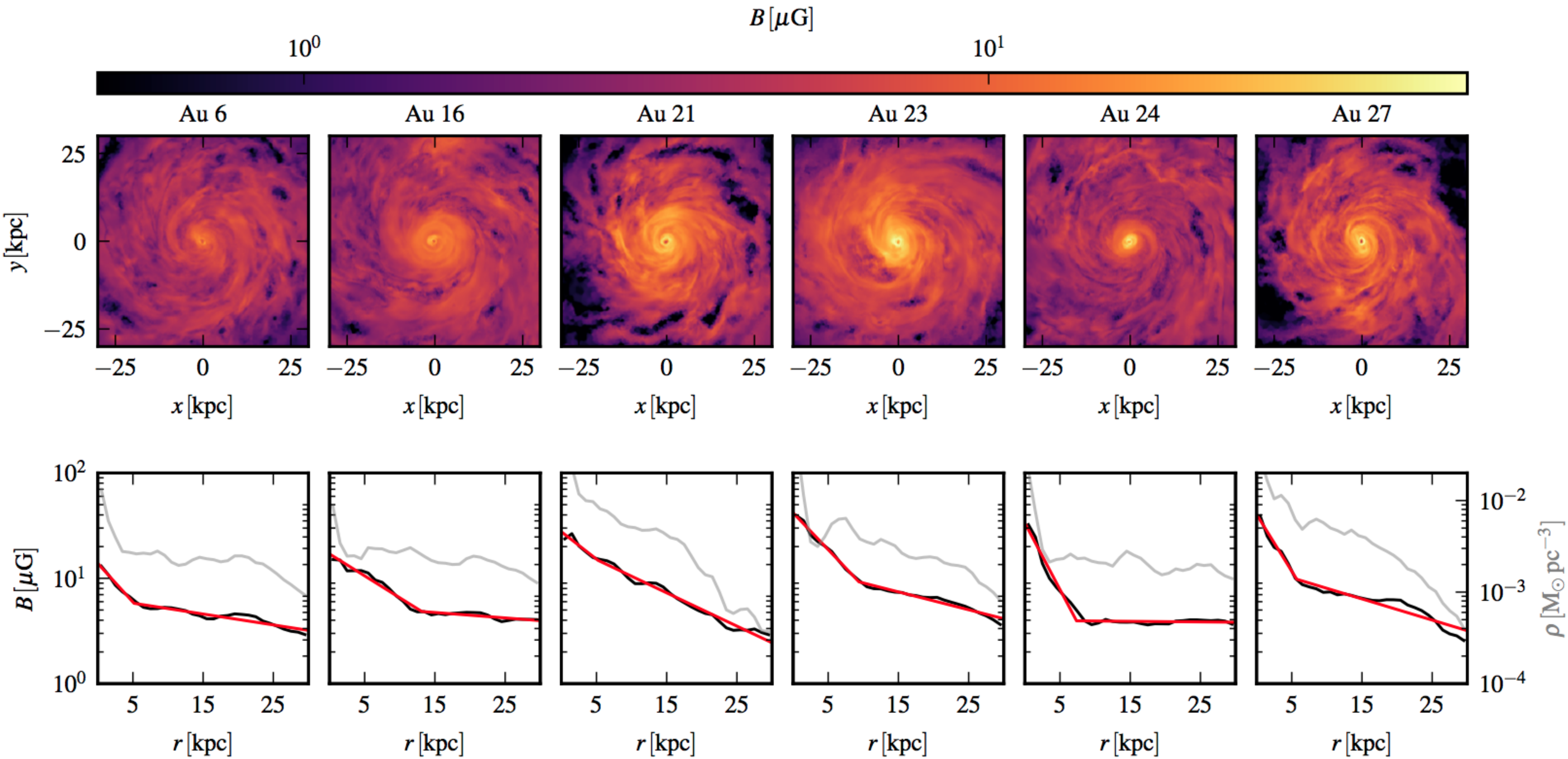

Pakmor et al. (2017)

There are also characteristic double power-law exponential profiles in the vertical direction

B-FIELD ENERGY DENSITY AND VERTICAL MAGNETIC PROFILES

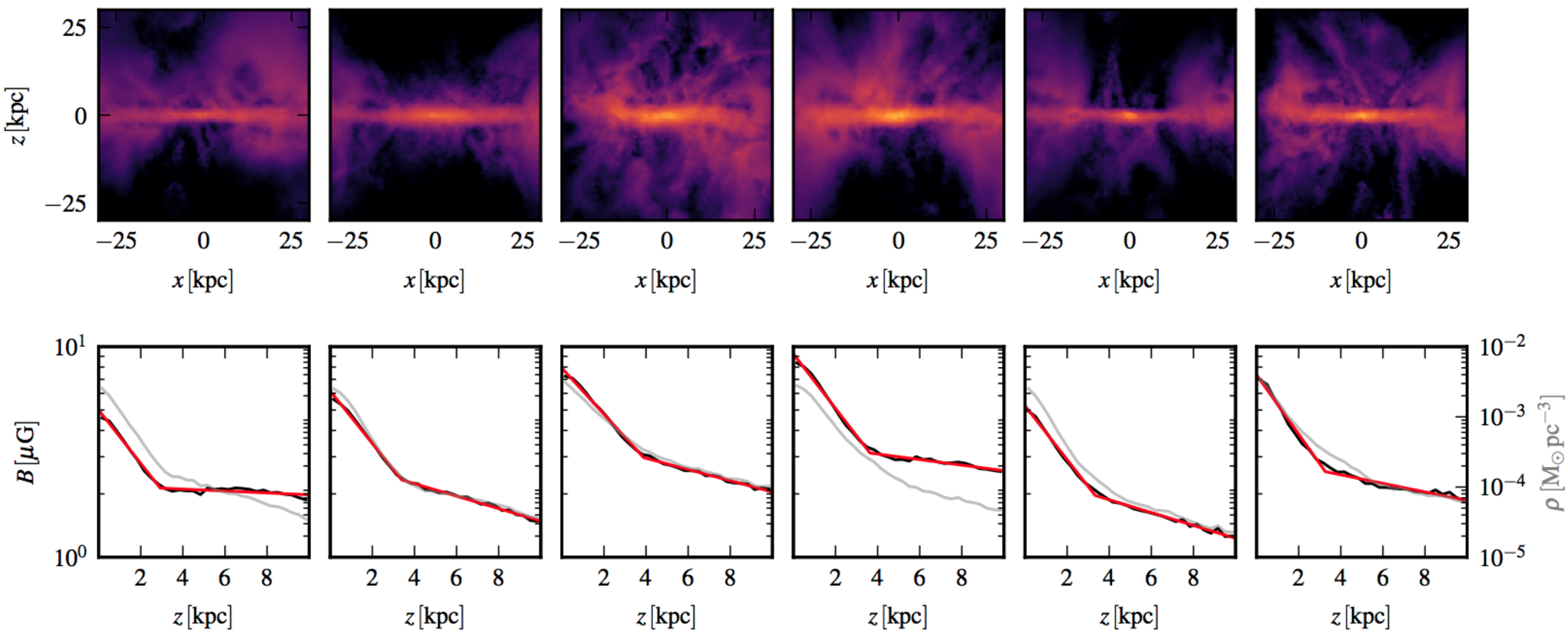

Pakmor et al. (2017)

The predicted magnetic field strength agrees quite well with observations

PROFILES OF MAGNETIC FIELD STRENGTH IN SIMULATIONS AND OBSERVATIONS

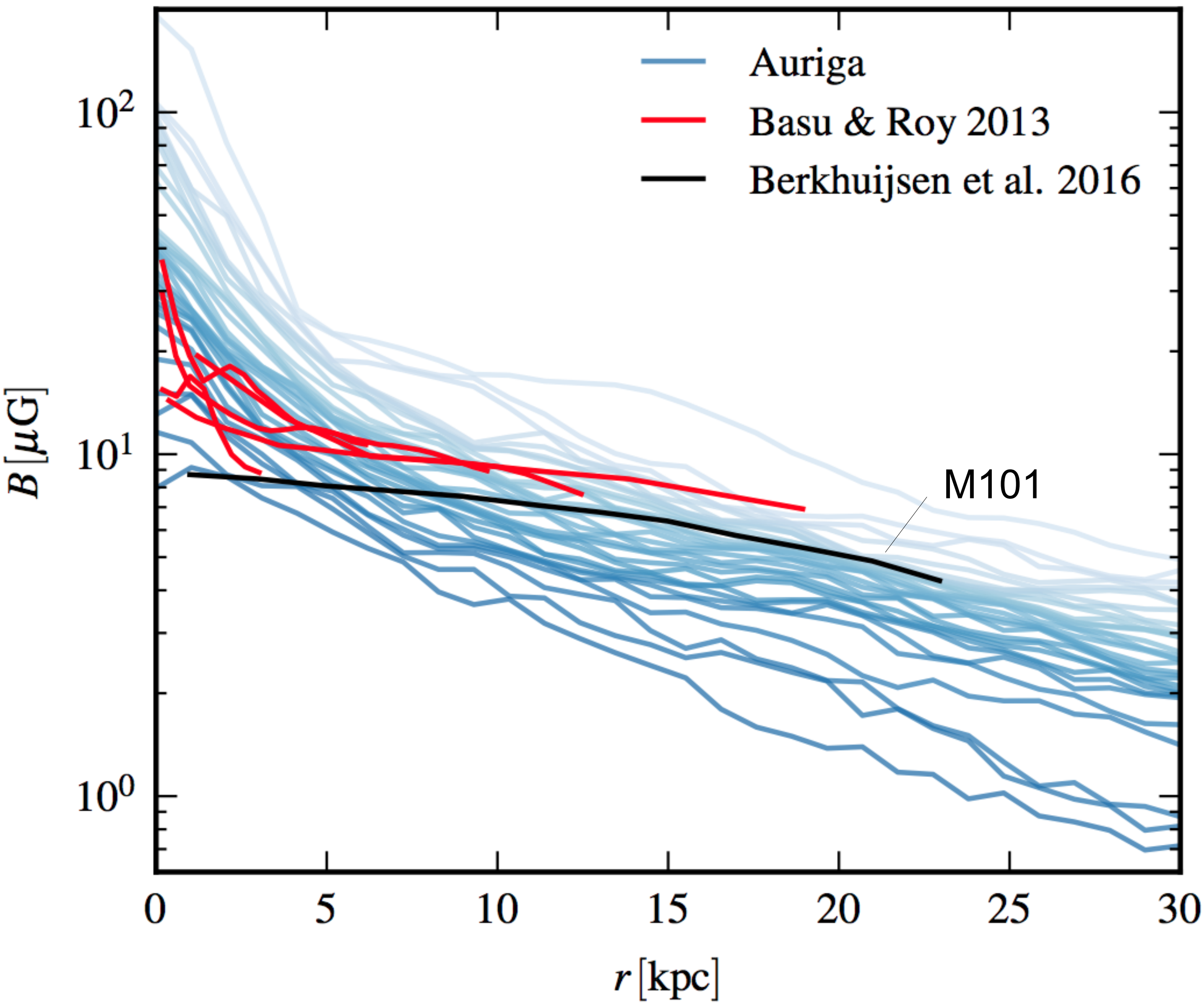

Pakmor et al. (2017)

Theres is little impact of magnetic fields on the star formation histories because equipartition is reached too late

COMPARISON OF SIMULATIONS WITH AND WITHOUT MAGNETIC FIELDS

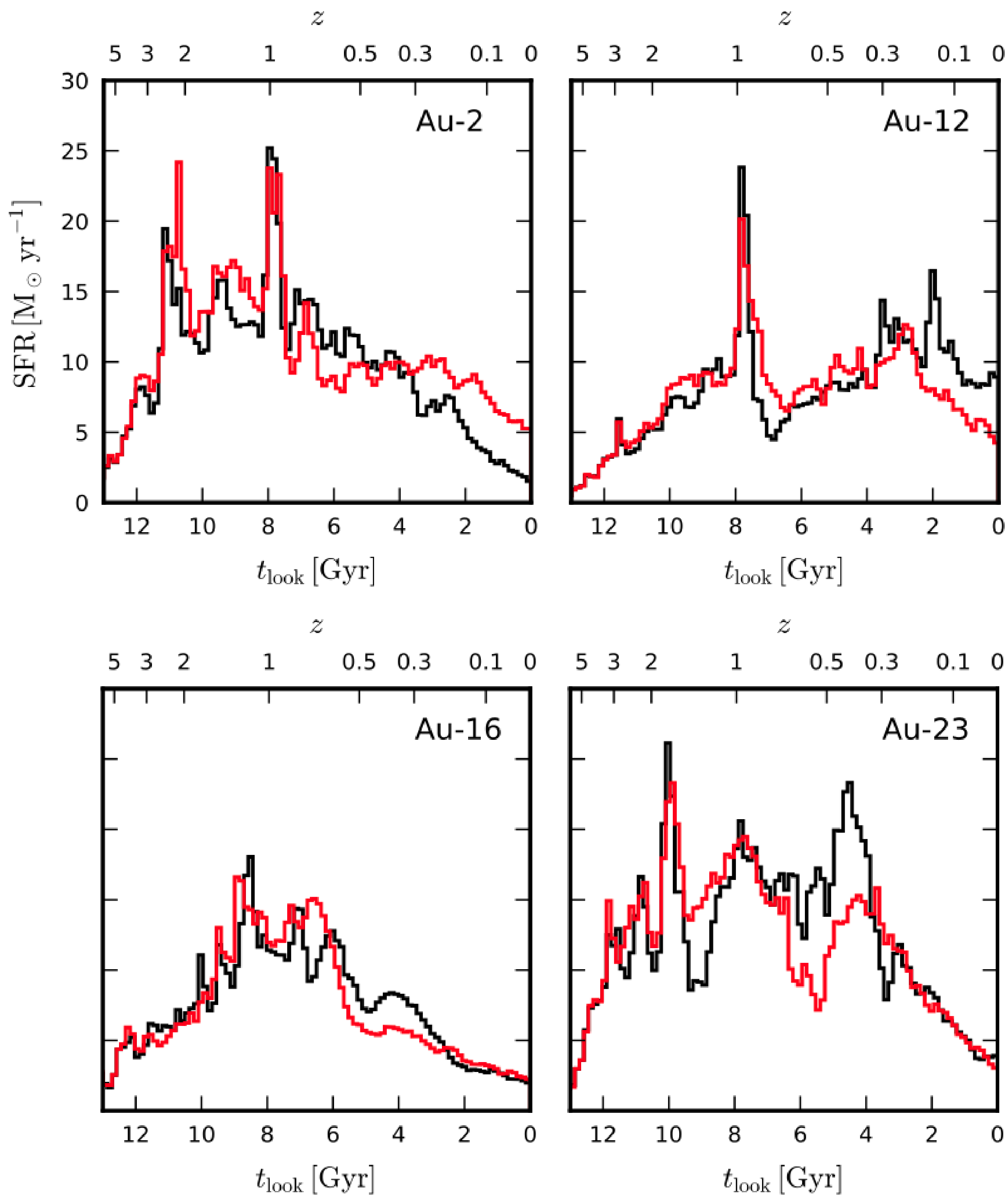

Black: with B-Fields

Red: without B-Fields

Pakmor et al. (2017)

Cosmic rays

The Galactic cosmic ray energy spectrum provides a significant contribution to the total ISM pressure

GLOBAL PROPERTIES OF GALACTIC COSMIC RAYS

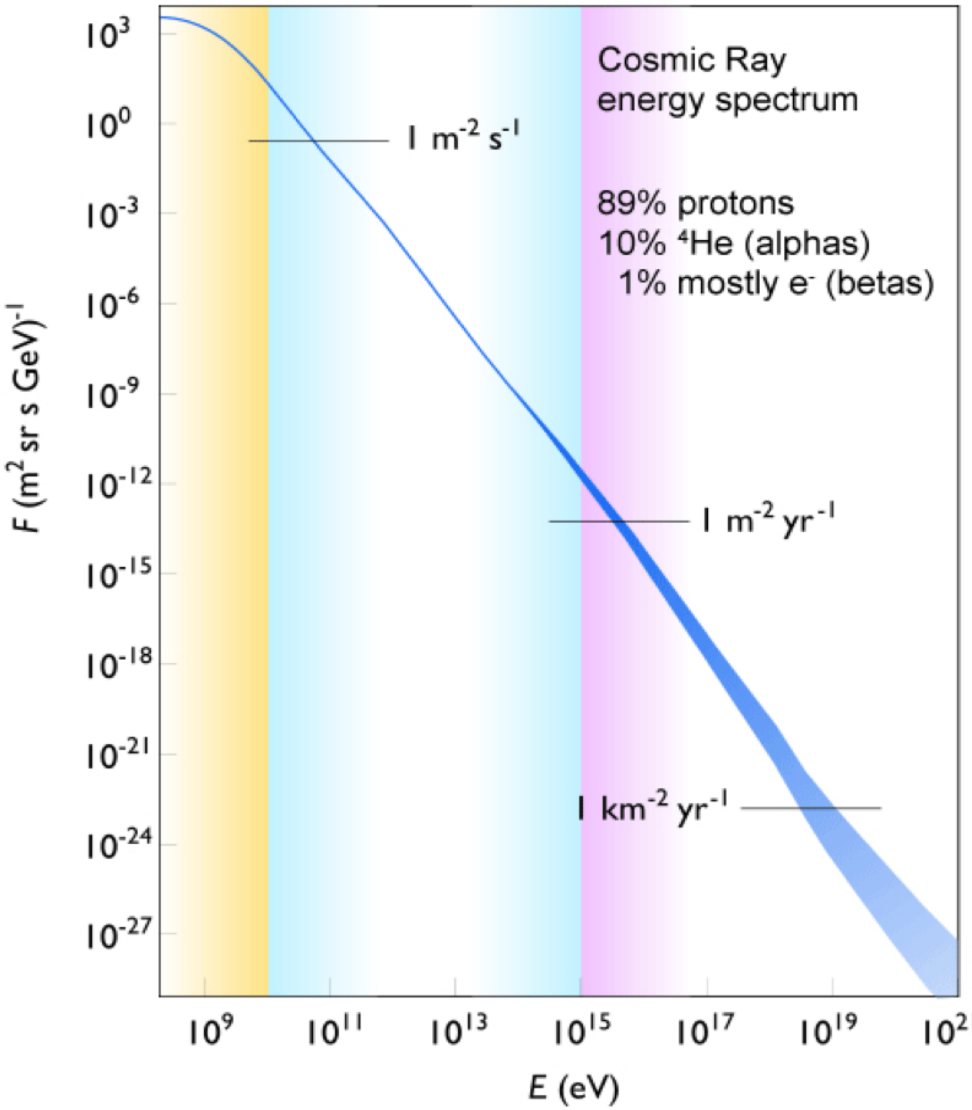

data compiled by Swordy

energy density in cosmic rays:
comparable to thermal and magnetic energy densities in ISM (equipartition)

main production mechanisms:

- supernova shocks (10-30% of the energy appears as CRs)
- large-scale structure formation shocks

main dissipation mechanisms:

- Coulomb losses
- hadronic interactions, mostly pion production
- Bremsstrahlung (negligible for protons)

CRs have a larger dissipation timescale than thermal cooling, and the softer equation of states keeps the pressure high in outflows

COMPARISON OF DISSIPATION TIMESCALES

Jubelgas et al. (2016)

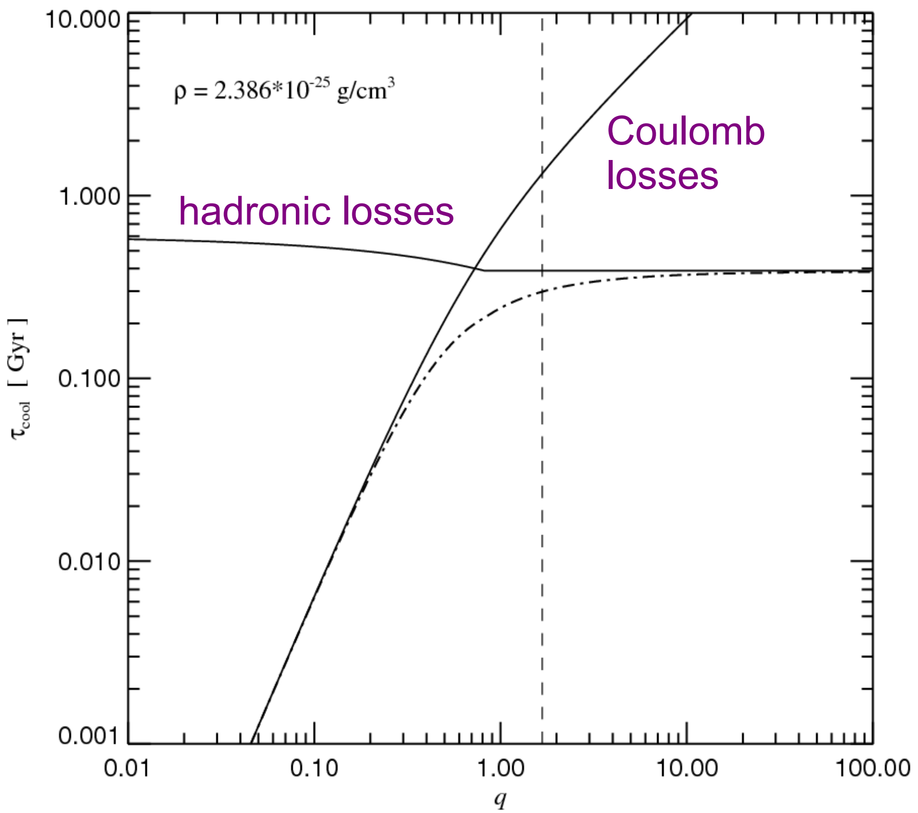

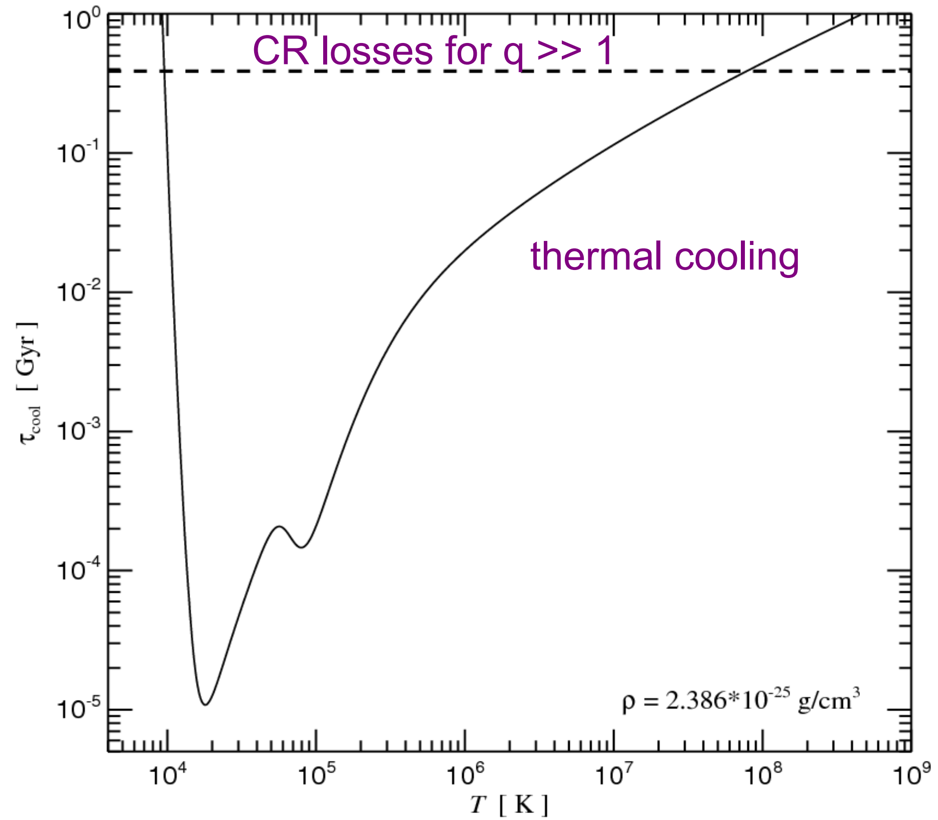

Also important: Softer equation of state, $P \sim \rho^{4/3}$ (buoyancy effects!)

And: CR dissipation dumped into thermal reservoir, increasing the pressure.

$$\Delta E/V = P/(\gamma - 1) = P_{cr}/(\gamma_{cr} - 1)$$

The CR dynamics is coupled to magnetic fields permeating the gas

INTERACTIONS OF COSMIC RAYS AND MAGNETIC FIELDS

Cosmic rays scatter on magnetic fields – this lets them exert a pressure on the thermal gas, and diffuse relative to its rest frame.

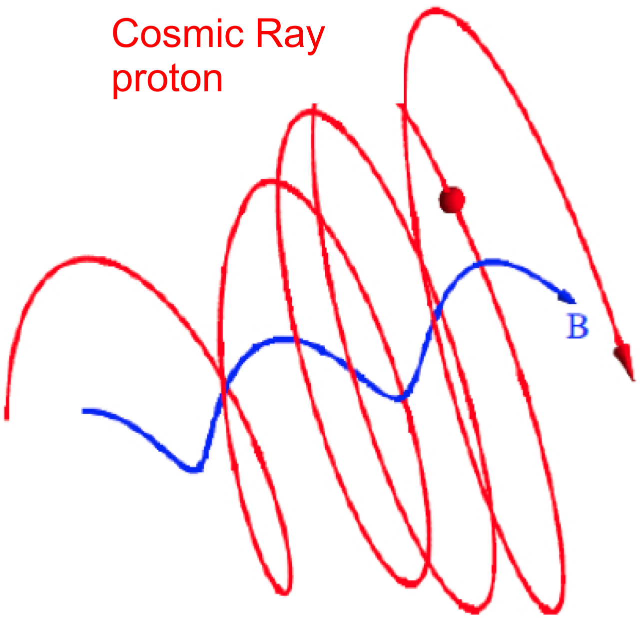

Streaming instability:

- CRs can in principle move rapidly along field lines (with c), which acts to reduce any gradient in their number density.
- But if $c_s > v_A$, CR excite Alfven waves (streaming instability)
- scattering off this wave field in turn limits the CR bulk speed to a much smaller, effective streaming speed v_{str}
- streaming speed: $\mathbf{v}_{\rm str} = -v_{\rm str}\dfrac{\nabla P_{\rm cr}}{|\nabla P_{\rm cr}|}$

$$v_{\rm str} = \lambda \max(c_S, v_A)$$
$$\lambda \sim 1$$

The CR transport complicates fluids dynamics considerable

COSMIC RAY DYNAMICS WITHOUT SOURCE AND SINK TERMS

$$\frac{\partial \boldsymbol{U}}{\partial t} + \nabla \cdot \mathbf{F} = \boldsymbol{S}$$

$$\boldsymbol{U} = \begin{pmatrix} \rho \\ \rho\boldsymbol{v} \\ \varepsilon \\ \varepsilon_{\rm cr} \\ \boldsymbol{B} \end{pmatrix}, \quad \mathbf{F} = \begin{pmatrix} \rho\boldsymbol{v} \\ \rho\boldsymbol{v}\boldsymbol{v}^{\rm T} + P\mathbf{1} - \boldsymbol{B}\boldsymbol{B}^{\rm T} \\ (\varepsilon + P)\boldsymbol{v} - \boldsymbol{B}\,(\boldsymbol{v}\cdot\boldsymbol{B}) \\ \varepsilon_{\rm cr}\boldsymbol{v} + (\varepsilon_{\rm cr} + P_{\rm cr})\boldsymbol{v}_{\rm st} - \kappa_\varepsilon \boldsymbol{b}\,(\boldsymbol{b}\cdot\nabla\varepsilon_{\rm cr}) \\ \boldsymbol{B}\boldsymbol{v}^{\rm T} - \boldsymbol{v}\boldsymbol{B}^{\rm T} \end{pmatrix}, \quad \boldsymbol{S} = \begin{pmatrix} 0 \\ \mathbf{0} \\ P_{\rm cr}\,\nabla\cdot\boldsymbol{v} - \boldsymbol{v}_{\rm st}\cdot\nabla P_{\rm cr} + \Lambda_{\rm th} + \Gamma_{\rm th} \\ -P_{\rm cr}\,\nabla\cdot\boldsymbol{v} + \boldsymbol{v}_{\rm st}\cdot\nabla P_{\rm cr} + \Lambda_{\rm cr} + \Gamma_{\rm cr} \\ \mathbf{0} \end{pmatrix}$$

$$P = P_{\rm th} + P_{\rm cr} + \frac{\boldsymbol{B}^2}{2} \qquad \varepsilon = \varepsilon_{\rm th} + \frac{\rho\boldsymbol{v}^2}{2} + \frac{\boldsymbol{B}^2}{2} \qquad \boldsymbol{v}_{\rm st} = -\frac{\boldsymbol{B}}{\sqrt{\rho}}\,{\rm sgn}(\boldsymbol{B}\cdot\nabla P_{\rm cr})$$

cosmic ray streaming,
nasty(!) numerically

Energy equation:

$$\frac{\partial \varepsilon_{\rm cr}}{\partial t} + \nabla\cdot\left[\varepsilon_{\rm cr}(\boldsymbol{v}+\boldsymbol{v}_{\rm st}) - \underbrace{\kappa_\varepsilon \boldsymbol{b}\,(\boldsymbol{b}\cdot\nabla\varepsilon_{\rm cr})}_{\text{anisotropic diffusion}}\right] = -P_{\rm cr}\,\nabla\cdot(\boldsymbol{v}+\boldsymbol{v}_{\rm st}) + \Lambda_{\rm cr} + \Gamma_{\rm cr}$$

Cosmic ray production at shocks slows the shock speed

SLICES THROUGH A SPHERICAL BLAST WAVE

$\zeta = 0.5$

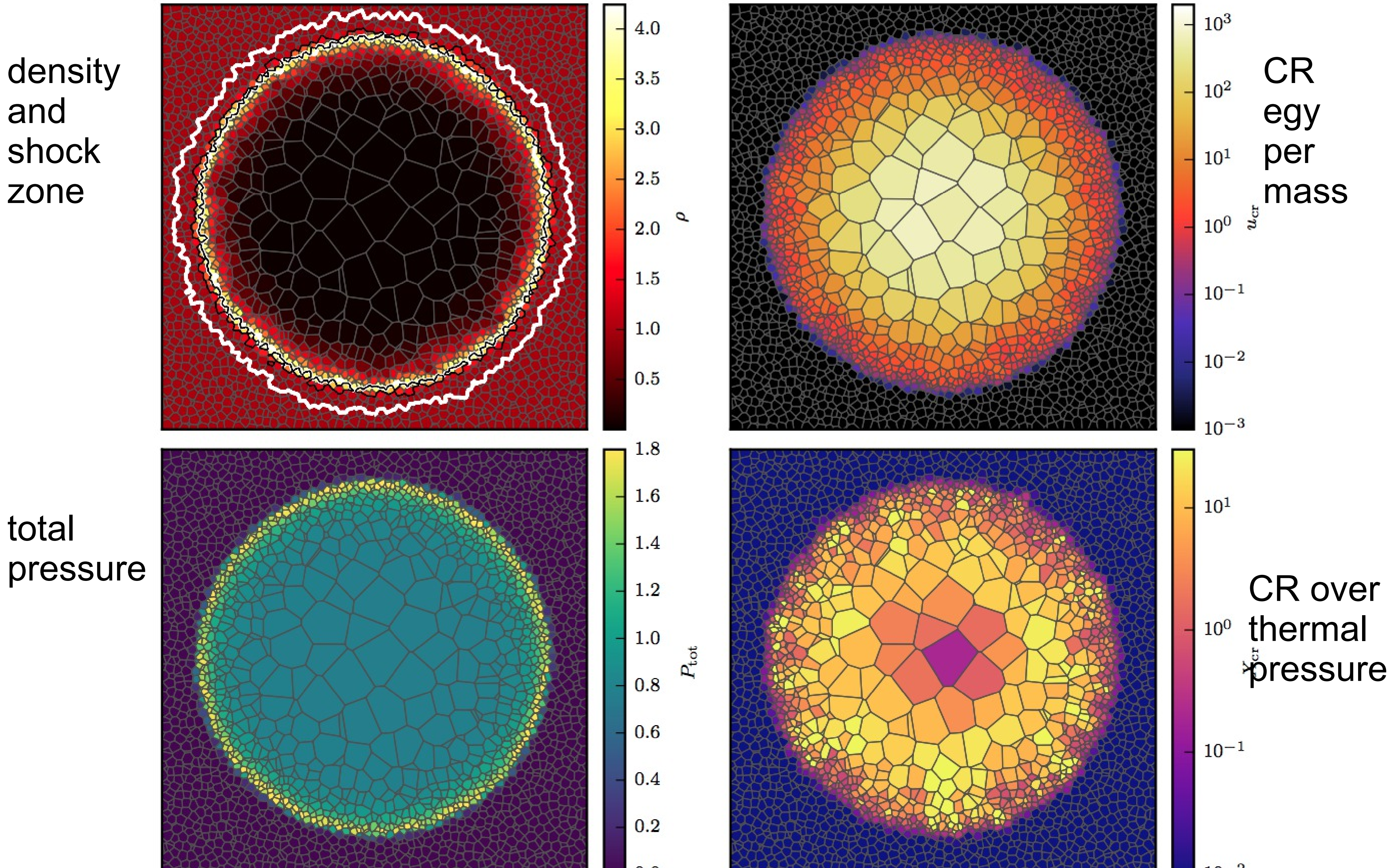

Pfrommer et al. (2016)

The entropy constraint can be easily violated in many simple linear discretization schemes for anisotropic transport

THE TROUBLE WITH THE B-FIELD DIRECTION

Example: Thermal conduction

$$\boldsymbol{j} = -\kappa \boldsymbol{b}(\boldsymbol{b} \cdot \nabla T) \qquad \rho \frac{\mathrm{d}u}{\mathrm{d}t} + \nabla \cdot \boldsymbol{j} = 0$$

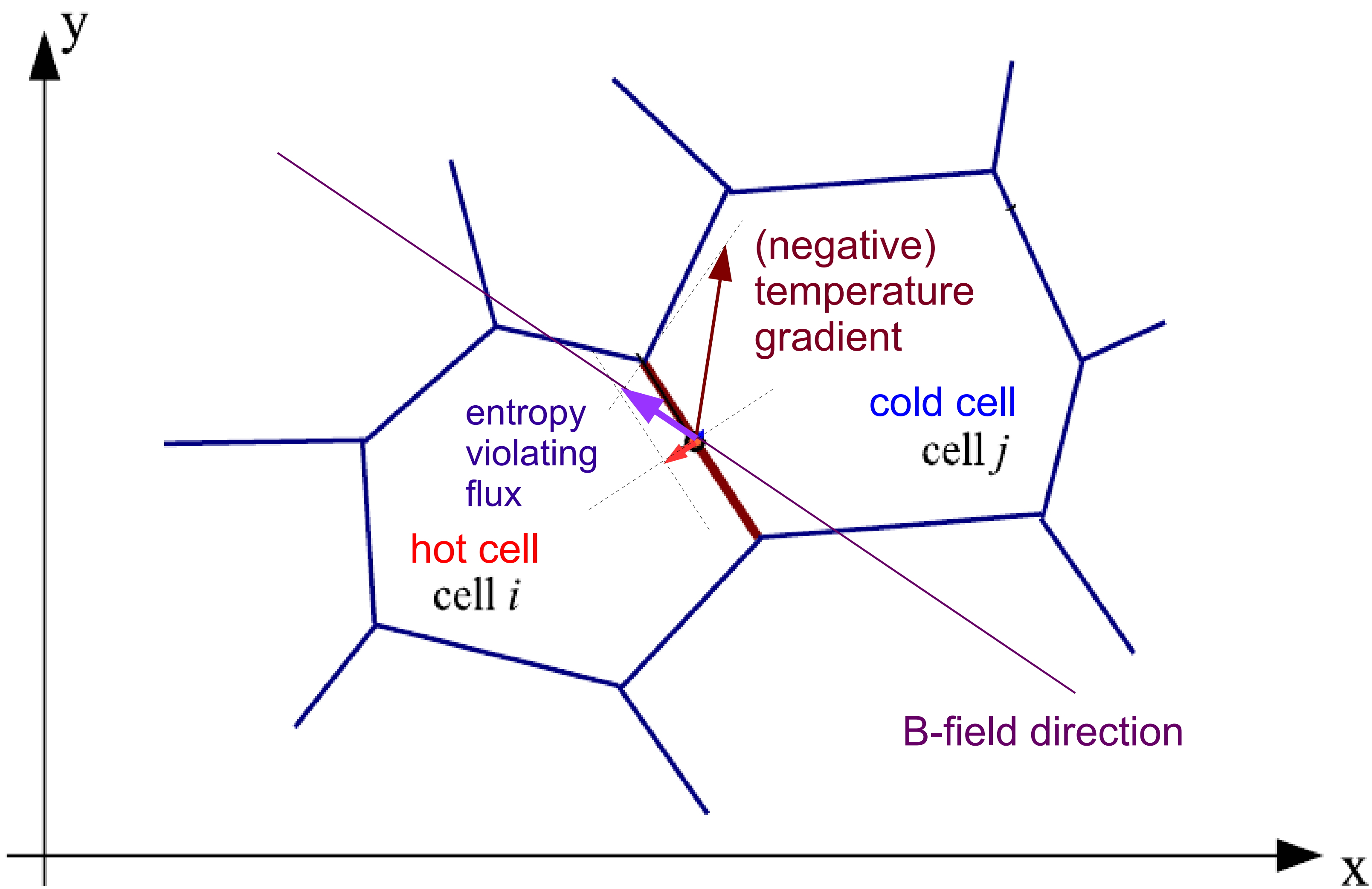

We have developed two independent solvers for anisotropic transport that perform very similarly

SEMI-IMPLICIT METHODS IN AN UNSTRUCTURED MESH

Pakmor et al. (2016)

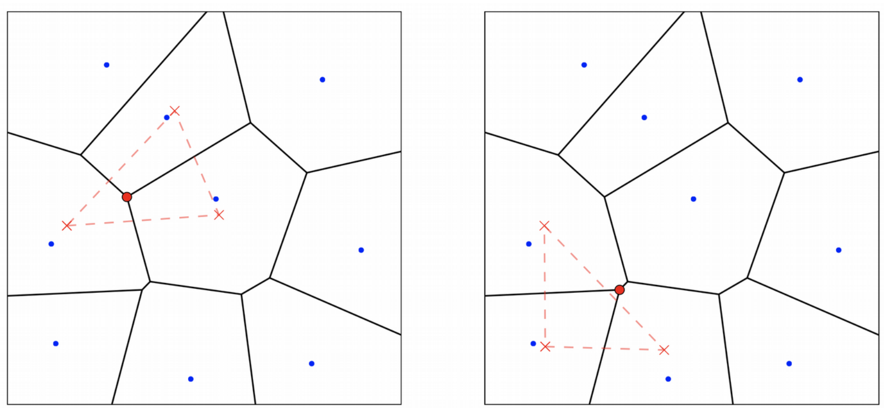

corner-based gradient estimates

- conservative
- does not violate entropy constraint
- allows for semi-implicit integration with individual timesteps
- multi-grid accelerated iterative solver (HYPRE/GMRES) with algebraic preconditioner

Kannan et al. (2016)

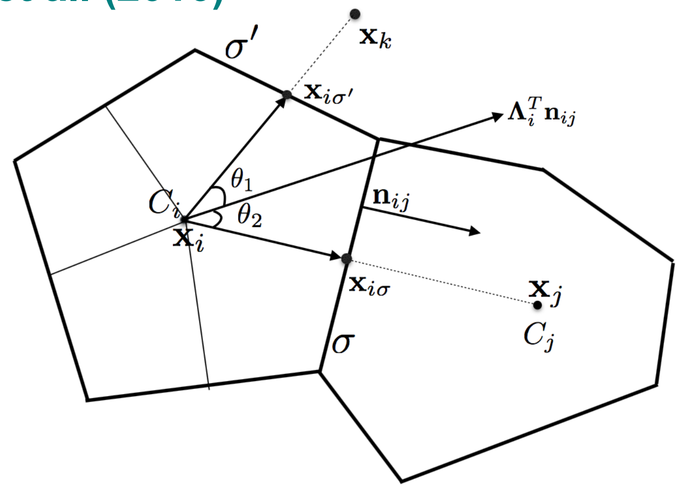

one-sides flux with harmonic averaging points

- oblique fluxes being limited such that the total flux is both l cally conservative and extremum preserving
- semi-implicit integration in time
- only compact stencil needed

Semi-implicit anisotropic transport of CRs with individual timesteps on an unstructured mesh

CONVERGENCE STUDY OF THE “RING TEST”

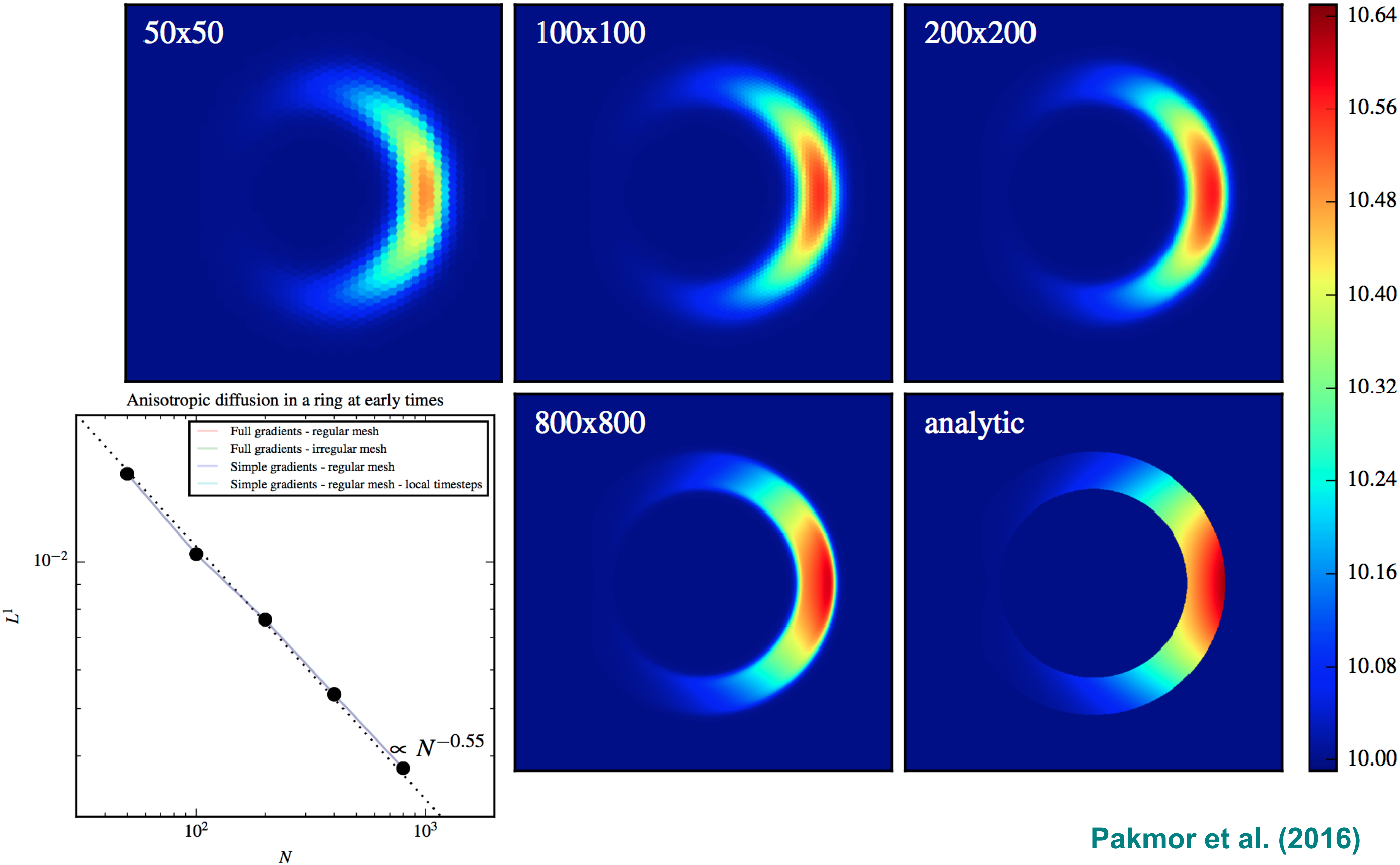

Pakmor et al. (2016)

Transport processes of CRs are critical for driving winds

COMPARISON OF DISK GALAXY EVOLUTION WITH DIFFERENT COSMIC RAY PHYSICS

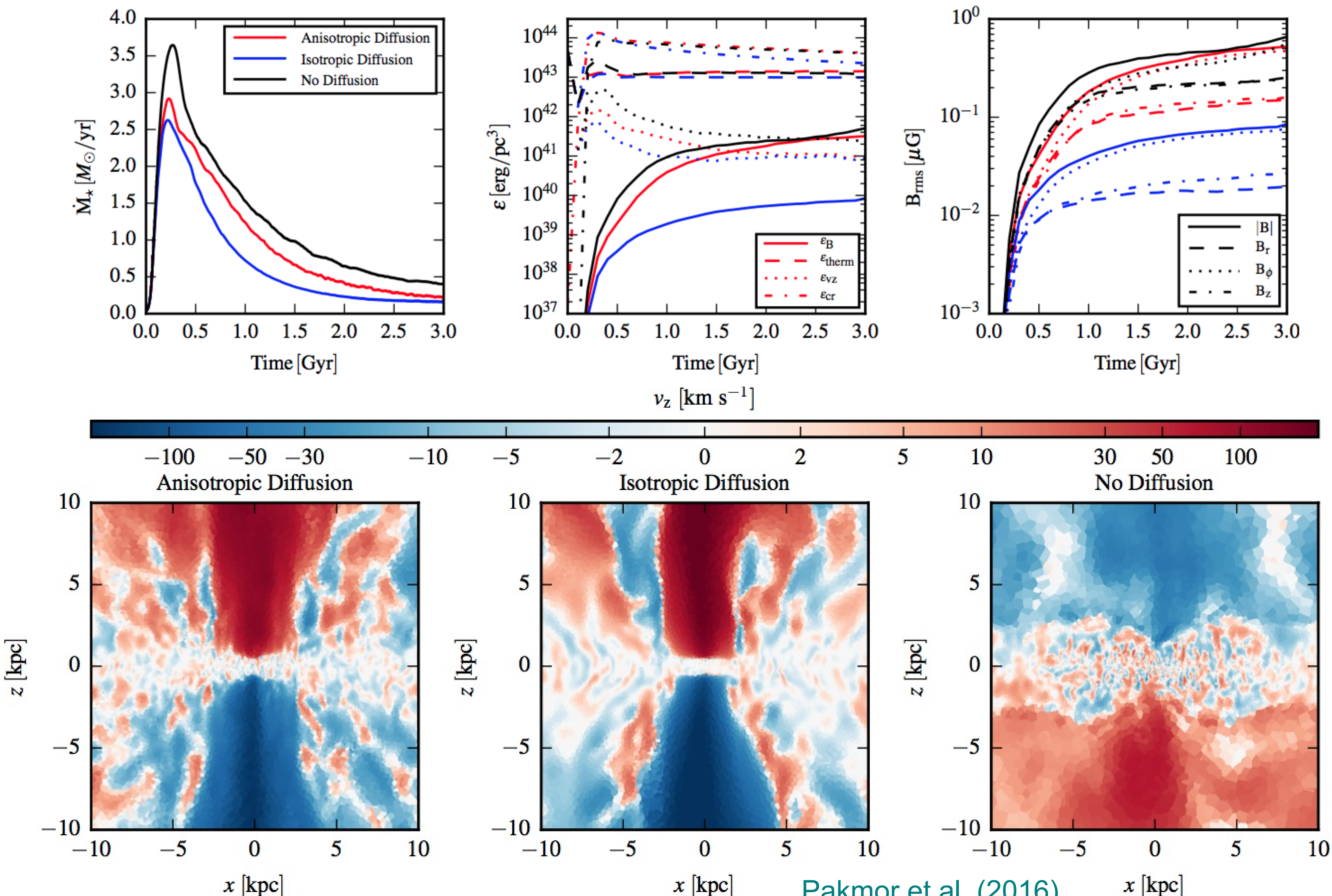

Pakmor et al. (2016)

The runs with isotropic diffusion slow down the galactic dynamo

FIELD AMPLIFICATION IN RUNS WITH ISOTROPIC AND ANISOTROPIC DIFFUSION

Dynamo in axisymmetric disk:
(neglecting Ohmic diffusion)

$$\frac{\partial \bar{B}_r}{\partial t} = -\frac{\partial}{\partial z}\left(\bar{v}_z \bar{B}_r + \mathcal{E}_\phi\right)$$

$$\frac{\partial \bar{B}_\phi}{\partial t} = -\frac{\partial}{\partial z}\left(\bar{v}_z \bar{B}_\phi + \mathcal{E}_r\right) + q\Omega_0 \bar{B}_r$$

Shukurov et al. (2006)

All terms similar, except that the gradients in the strength of the radial and vertical magnetic field are shallower for the isotropic diffusion run – this slows down the B-field amplification.

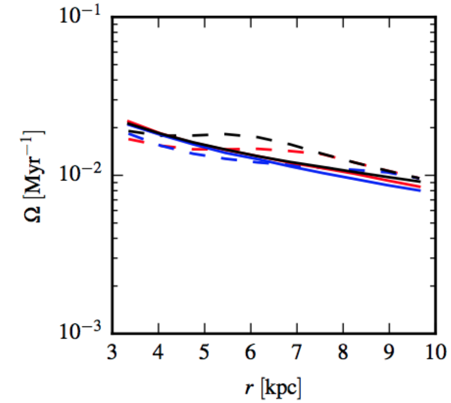

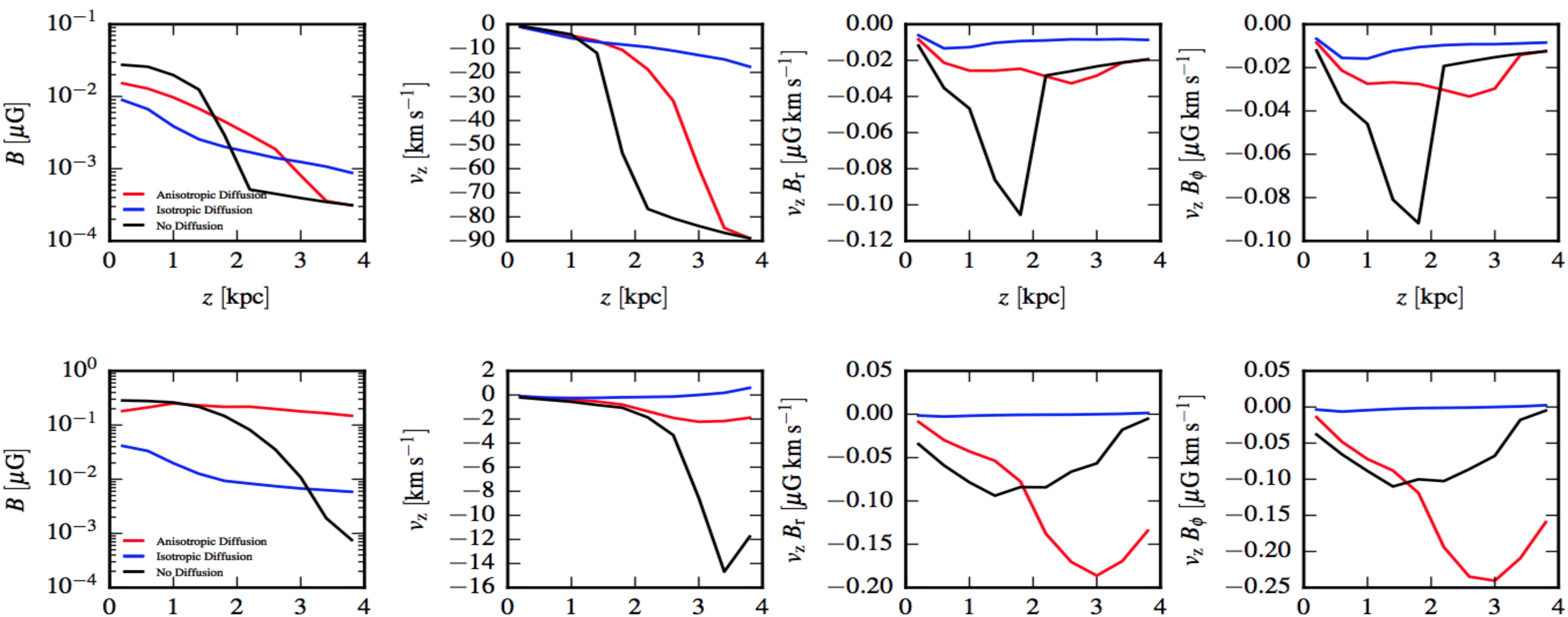

Pakmor et al. (2016)

Stratified-box simulations of SN feedback demonstrate the importance of CRs for driving outlows

DIFFERENT MODES OF SUPERNOVA FEEDBACK

with gas self-gravity and stationary stellar potential

self-shielding with TreeCol

$$\Sigma_0 = 10\ \mathrm{M}_\odot\ \mathrm{pc}^{-2}$$
$$f_g = 0.1$$
$$m_t = 10\ \mathrm{M}_\odot$$
$$\varepsilon = 0.165\ \mathrm{pc}$$

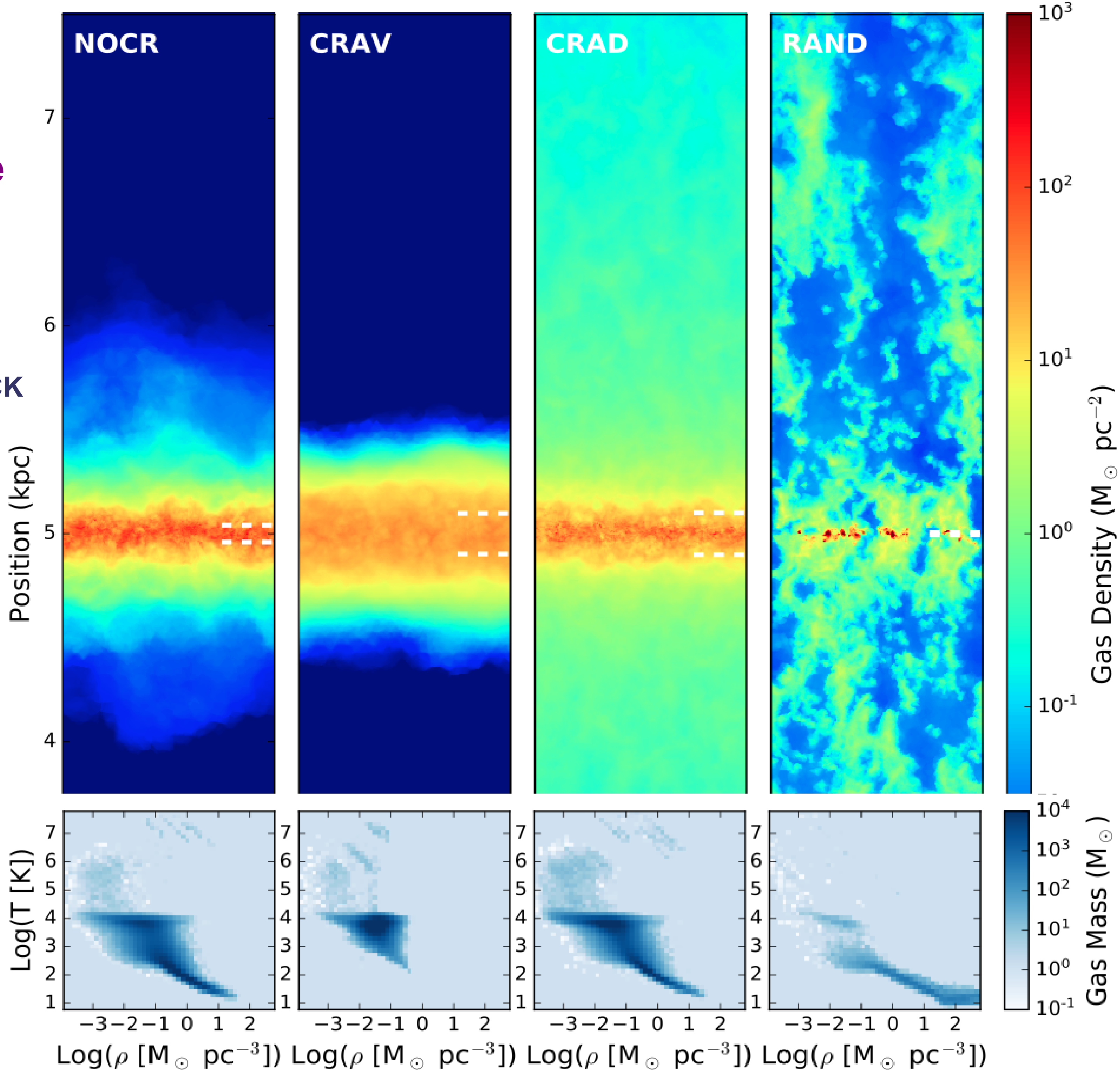

Simpson et al. (2016)

Cosmic ray transport processes reduce the star formation and sustain mass loaded winds

COMPARSON OF THE TIME EVOLUTION FOR DIFFERENT FEEDBACK MODELS

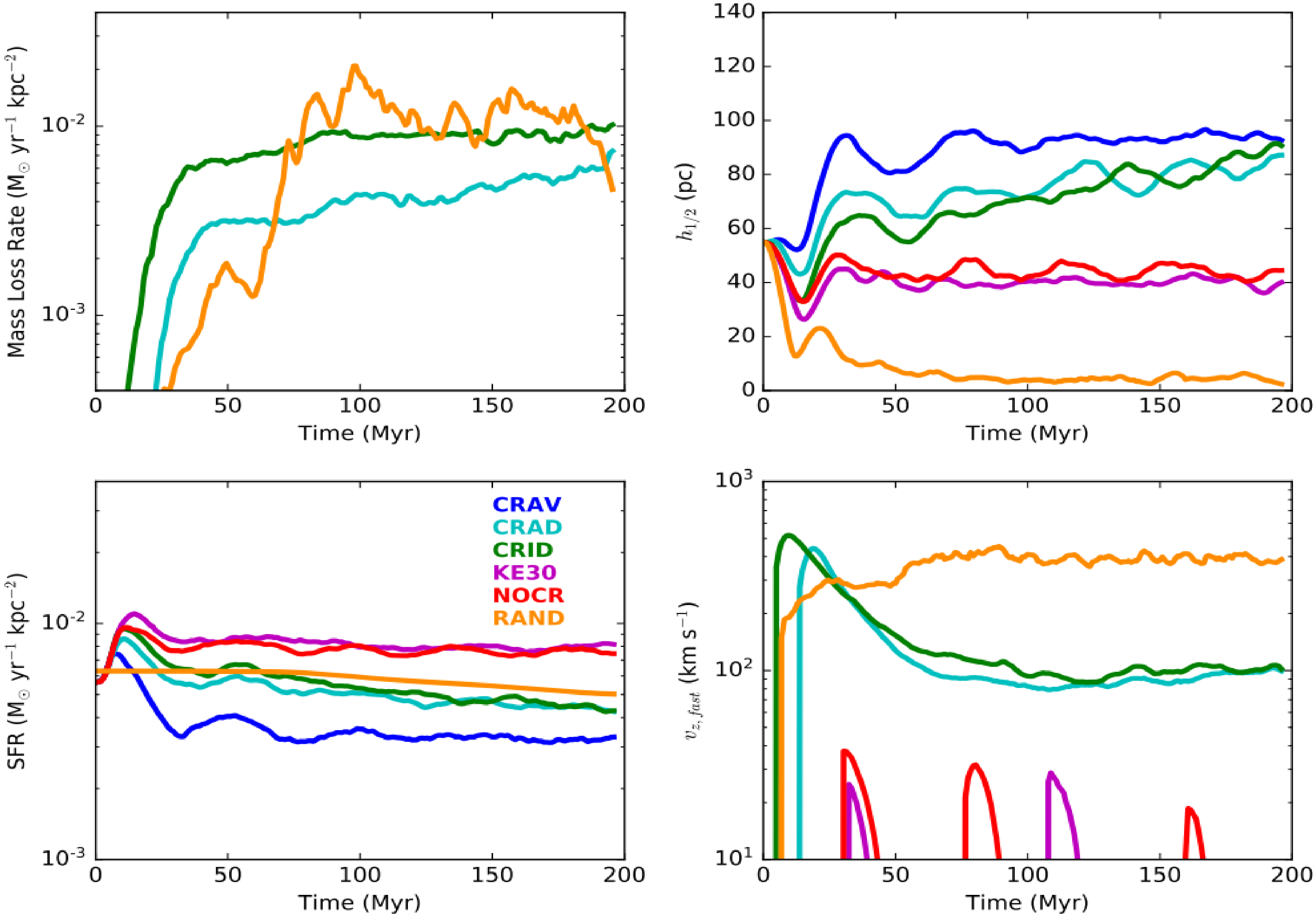

Simpson et al. (2016)

Summary: some progress but lots of open questions

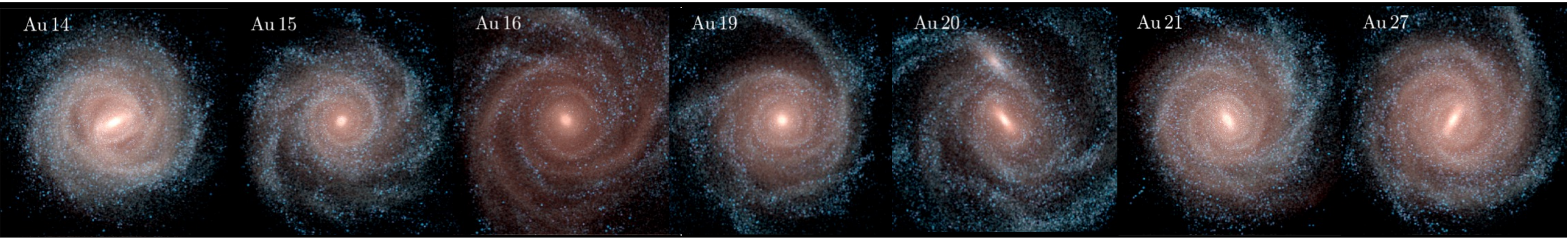

- Hydrodynamical cosmological simulations in ΛCDM produce **disk galaxies similar to the Milky Way**
- The **physical nature of the dominant feedback processes** is still highly uncertain: SN, cosmic rays, radiation pressure, black holes – which one is most critical?
- **Magnetic fields are efficiently amplified already at high-z** in a small-scale dynamo. Predicted properties at low redshift are consistent with observations.